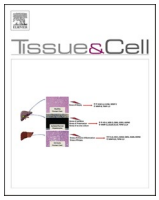
Tissue and Cell 91 (2024) 102544



Contents lists available at ScienceDirect

Tissue and Cell

journal homepage: www.elsevier.com/locate/tice



Endoplasmic reticulum stress of endometrial mesenchymal stem cells in endometriosis

Selenay Furat Rencber [a,b,c], Yusufhan Yazır [a,b,c,*], Mehmet Sarıhan [d], Zehra Sezer [f], Zeynep Ece Utkan Korun [b,e], Ahmet Ozturk [a,b,c], Gokhan Duruksu [b,c], Elif Guzel [f], Gurler Akpınar [d], Aydın Corakci [g]

[a] Department of Histology and Embryology, Faculty of Medicine, Kocaeli University, Kocaeli, Turkey
[b] Department of Stem Cell, Institute of Health Sciences, Kocaeli University, Kocaeli, Turkey
[c] Center for Stem Cell and Gene Therapies Research and Practice, Kocaeli University, Kocaeli, Turkey
[d] Department of Medical Biology, Faculty of Medicine, Kocaeli University, Kocaeli, Turkey
[e] Department of Obstetrics and Gynecology, Faculty of Medicine, Yeditepe University, İstanbul, Turkey
[f] Department of Histology and Embryology, Cerrahpasa Faculty of Medicine, Istanbul University-Cerrahpasa, Istanbul, Turkey
[g] Department of Obstetrics and Gynecology, Faculty of Medicine, Kocaeli University, Kocaeli, Turkey

ARTICLE INFO

Keywords:
Endometriosis
Endoplasmic reticulum stress
Mesenchymal stem cells
Infertility
Autophagy
Apoptosis

ABSTRACT

Objective: The human endometrium has significant regenerative abilities due to stem cells, which are vital in immunomodulation, immune tolerance, steroid hormone response, and inflammation. Endometriosis, an inflammatory gynecological disorder where endometrium-like tissue grows outside uterus, affects millions of women and often causes infertility. Recent research indicates that stem cells contribute to pathology of endometriosis. ER stress is implicated in various diseases, including endometriosis. This study aims to examine ER stress in eMSCs within endometriosis pathogenesis and uncover underlying disease mechanisms.
Methods: Samples were collected from healthy subjects and women with endometriosis in both proliferative and secretory phases. eMSCs were isolated and characterized via flow cytometry. ER stress protein levels were assessed using proteomic analysis, with validation through Western Blot and immunofluorescence staining. Gene expression was analyzed by RT-qPCR, and ultrastructural examination of eMSCs was conducted using TEM. ER stress markers in tissue samples were detected in SUSD2+ eMSCs through immunofluorescence staining and visualized using a confocal microscope. Statistical analysis was performed using SPSS program.
Results: The proteomics analysis uncovered ER stress-related proteins (DDRGK1, RTN3, ERp44, TMED2, TMEM33, TMX3) whose levels were significantly distinct from control group. Western Blot analysis and immunofluorescence staining results at protein level; RT-qPCR results at gene level supported these findings. TEM analysis also showed ultrastructural presence of ER stress in endometriosis groups.
Conclusion: Presence of ER stress in eMSCs in pathogenesis of endometriosis has been demonstrated using various methods. Our research has potential to shed light on pathology of endometriosis and offer promising avenues for non-invasive diagnosis and potential treatment.

1. Introduction

Endometriosis is a common, inflammatory, benign, gynecological disease that involves the presence and growth of dysfunctional endometrial-like glands and stroma with reactive fibrosis, often outside the uterus (Clement, 2007). This disease, which affects millions of women, is the most important cause of infertility and pelvic pain (Lessey and Kim, 2017) and is seen in approximately 10 % of women of reproductive age and 20–50 % of infertile women (Ekiz-Yilmaz et al., 2021). Although endometriotic lesions are mostly seen in the pelvic peritoneum and ovary, they have also been detected rarely in the pericardium, pleura, lung parenchyma and brain (Hufnagel et al., 2015). Current approaches are not effective in the treatment of the disease, and the recurrence rate is approximately 50 % in the first 5 years after the lesion(s) are removed (He et al., 2016).

Studies on the pathology of endometriosis have mostly focused on

* Corresponding author at: Department of Histology and Embryology, Faculty of Medicine, Kocaeli University, Kocaeli, Turkey.
E-mail address: yusufhanyazir@yahoo.com (Y. Yazır).

https://doi.org/10.1016/j.tice.2024.102544
Received 22 July 2024; Received in revised form 26 August 2024; Accepted 27 August 2024
Available online 28 August 2024
0040-8166/© 2024 Published by Elsevier Ltd.

mature cells in the endometrium, but the mechanism underlying this pathology has not been fully explained to date. Especially in recent years, findings have been revealed that endometrial stem cells (eMSC) cause the etiology of endometriosis (Pluchino and Taylor, 2016). According to this hypothesis, eMSCs shed from the eutopic endometrium with menstruation are transferred to the peritoneum or peritoneum-related areas with retrograde menstruation. The hypothesis is strongly supported by the fact that women with endometriosis shed more basalis fragments (the layer where stem cells are more dense) during menstruation compared to women without endometriosis (Cousins *et al.*, 2018; Hufnagel et al., 2015; Liu et al., 2020). This is further demonstrated by the presence of eMSCs in menstrual blood (Liu et al., 2020) and endometriotic lesions, as well as the detection of stem cell genes such as OCT4, SOX2, NANOG, Musashi, and c-KIT in these lesions. Additionally, studies have shown increased proliferation, migration, invasion, and angiogenesis activity of ectopic eMSCs compared to eutopic ones (Gargett et al., 2016).

Besides, it has been observed that ectopic MSCs exhibit distinct immunophenotypic properties as compared to healthy eutopic MSCs. Research has revealed that the expression of toll-like receptor, collectin, proinflammatory factors, angiogenesis, and migration-related factors is elevated in these cells (Liu et al., 2020). Gene microarray studies have indicated that progesterone resistance observed in endometriosis is transmitted to endometrial stromal fibroblasts from eMSCs (Barragan et al., 2016). This finding implies that the source of the disorder in decidual differentiation is attributable to eMSCs (Cousins et al., 2018). It has been reported that the abnormal presence of dysfunctional endometriotic stem cells in the eutopic endometrium may disrupt the epithelial-stromal polarity, leading to decreased endometrial receptivity in patients with endometriosis (Macer and Taylor, 2012).

The endoplasmic reticulum (ER) is a cellular organelle that plays a critical role in several essential cellular functions, such as protein synthesis, folding, modification, trafficking, and calcium storage (Guzel et al., 2017). Misfolded/unfolded proteins, increased or decreased protein degradation creates a stress in the cell, and this stress is detected by various chaperone sensors (especially GRP78) in the ER and activates the unfolded protein response (UPR). In the UPR, folding capacity of unfolded proteins that accumulate in the ER lumen and the synthesis of accessory molecules that supports folding are increased, and misfolded proteins (if not corrected) are sent for degradation to reduce the ER load. If the cell still cannot adapt, it is directed to apoptosis to prevent damage to the surrounding tissue (Oakes and Papa, 2015). It has been determined that disruptions in this protein homeostasis play a role in the pathogenesis of various diseases, including endometriosis (Guzel et al., 2017). When the relationship of UPR molecules and apoptosis-related molecules with endometriosis is examined; Bcl-2 and Bcl-xL expression is higher in ectopic endometrium than in eutopic and healthy endometrium (Delbandi et al., 2020), GRP78 and CHOP expression is lower in the late secretory phase than in healthy endometrium (Choi et al., 2019). It has been reported that GRP78 and xBP1 expression levels are higher in endometrium than in ectopic endometrium, CHOP expression does not change, and ATF6 is expressed more in eutopic and ectopic endometrium than in healthy endometrium (Ciavattini et al., 2018). It has also been reported that IKK suppresses apoptosis in endometriotic cells by phosphorylating Bad, which is a Bcl-2 antagonist (Kocbek et al., 2016). In the study conducted by Liang *et al.*, it was reported that the suppression of proliferation and increase of apoptosis in endometriotic stromal cells depend on JNK activation (Liang et al., 2017).

The present study aimed to investigate the association between eMSCs and ER stress in endometriosis pathology and elucidate the underlying mechanism of action. For this purpose, eMSCs were isolated from endometrial samples and characterized by flow cytometry, and then ER stress proteins whose expression level differed compared to the control group were identified via proteomics analysis. In the second step, these proteins were determined by western blot (WB) and immunofluorescence (IF) methods and encoding genes were analyzed by RT-qPCR. Also ER stress in these cells was examined ultrastructurally with transmission electron microscopy (TEM). In the endometrial tissue sections, Haematoxylin & Eosin (H&E) staining was performed for histological evaluation and last menstrual period (LMP) determination. Besides, ER stress markers was detected by immunoflorescense staining in SUSD2+ eMSCs in endometrial tissues via confocal microscope. Statistical analysis was performed with the SPSS program.

2. Materials and Methods

2.1. Patients

The endometrial tissues of the patients who were operated for benign gynecological conditions were accepted as the control group (n=7; aged 40–44 years, mean 42± 1,29). In the experimental group, endometrial (n=7; aged 39–44 years, mean 41±2,19) and endometriotic (n=13; aged 28–45 years, mean 37±8,64) samples were collected from women with endometriosis (specifically ovarian endometrioma). The menstrual cycle phases of the volunteers were determined and then subclassified into proliferative (days 1–14) and secretory phases (days 15–28) groups to observe the behaviour of eMSCs with regards to ER stress during different stages of the menstrual cycle (Choi et al., 2018).

The endometrium samples of the experimental group consisted of eutopic and ectopic endometrium of patients who were diagnosed with endometriosis as a result of laparoscopic and pathological examination. Participants in the control group who had regular menstrual cycles and undergone laparoscopy or hysterectomy for benign gynecological conditions, did not exhibit any endometriotic lesions as carefully evidenced by a gynecological surgeon. None of the volunteers were on or had received any hormonal or immunomodulatory treatments within three months before surgery. Patients with adenomyosis, pelvic inflammatory disease, malignancy, or autoimmune disorders were excluded from the study (Cao et al., 2017; Choi et al., 2019).

Eutopic endometrial samples from healthy and endometriosis groups were primarily obtained from patients who underwent total abdominal hysterectomy and bilateral salpingo-oophorectomy (TAH+BSO) procedures. Ectopic endometrial (endometriotic) samples, on the other hand, were obtained from patients who underwent TAH+BSO and/or lesion excision procedures. The majority of the eutopic and ectopic endometrial samples were taken from the same patient but the others were not. To prevent damaging to the endometrium by taking samples, eutopic endometrial samples were not collected from patients with endometriosis (except for individuals who underwent TAH+BSO operation). At the end of the flow cytometry analysis, samples belonging to the same groups were pooled to eliminate age differencies and to provide more accurate results.

2.2. Study design

All tissue samples were divided into three pieces: Those to be used in *in vitro* experiments were taken into Hank's balanced salt solution (HBSS) and quickly transferred (Choi et al., 2019) to Kocaeli University Stem Cell and Gene Therapies Research and Application Center (KOGEM) laboratories. The samples to be used for histochemistry and immunohistochemistry experiments were fixed in 10 % neutral buffered formalin solution for tissue processing.

2.3. Endometrial and endometriotic eMSC isolation

Control, eutopic and ectopic endometrial tissue samples were mechanically divided into 1–2 mm^3 pieces; then incubated in a solution containing HBSS, Fetal Bovine Serum (FBS), penicillin-streptomycin and collagenase enzyme in a 37ºC water bath for 60–90 minutes. Then, cell aggregates and epithelial cells were removed from the medium by passing them through filters with 100-, 70-, and 40- μm pore diameters,

respectively. The obtained endometrial cells were cultured in flasks containing Dulbecco's Modified Eagle Medium: Nutrient Mixture F-12 (DMEM/F12), 10 % FBS and 1 % penicillin-streptomycin (10,000c U/ml) medium. In Passage 3, the cells were characterized by flow cytometry method.

2.3.1. Flow cytometry

Following the passage 3, the eMSCs were collected and suspended in culture medium at a concentration of 1×10^6 cells/ml. We used 1×10^5 cells for each marker in characterization of eMSCs via flow cytometer. The flow cytometry process was carried out using the Becton Dickinson FACSCalibur instrument (BD Biosciences, USA), in accordance with the methodology outlined by Karaoz et al. (Karaoz et al., 2009). The data obtained were analyzed using the CellQuest software (BD Biosciences, USA).

Immunophenotyping characterization of MSCs was performed with antibodies against the following human antigens: CD34 PE (BD 345802; BD Biosciences, USA), CD44 (BD555478; BD Biosciences, USA), CD45 FITC (BD 55482; BD Biosciences, USA), CD140b PE (BD558821; BD Biosciences, USA), CD29 PE (BD 555443; BD Biosciences, USA), CD146 PE (BD 550315; BD Biosciences, USA), CD105 PE (BD 560839; BD Biosciences, USA), CD73 PE (BD 550257; BD Biosciences, USA), CD90 (555596; BD Biosciences, USA), CD31(555446; BD Biosciences, USA), and HLA-DR FITC (BD 340688; BD Biosciences, USA). The antigen selection was made based on MSC and eMSC defining criteria (Dominici et al., 2006; Gargett et al., 2016; Masuda et al., 2012). All antibodies were from BD Biosciences. More than 50 % staining was regarded as positive.

2.3.2. Ostegenic, adipogenic and chondrogenic differentiation of eMSCs

After flow cytometry analysis, adipogenic, chondrogenic and osteogenic differentiation was performed to elucidate MSC comfirmation (Polat et al., 2024; Ciuffreda et al., 2016; Zuk et al., 2002).

2.3.2.1. Osteogenic differentiation. After passage 3, eMSCs were cultured on a round glass coverslip using normal medium, with approximately 3×10^3 cells in 1 cm^2 of the culture dish. Afterwards, the cells were cultured with DMEM-F12 supplemented with osteogenic differentiation-inducing supplements (100 nM dexamethasone, 0.05 µM ascorbate-2-phosphate, 10 mM β-glycerophosphate, 1 % penicillin-streptomycin) and 10 % FBS. The differentiation medium was changed twice a week. At the end of 28 days, osteogenic differentiation was assessed by Alizarin Red staining (Karaoz et al., 2009).

2.3.2.2. Adipogenic differentiation. After passage 3, eMSCs were cultured on a round glass coverslip using normal medium, with approximately 3×10^3 cells in 1 cm^2 of the culture dish. Afterwards, the cells were cultured in DMEM-F12 medium containing adipogenic differentiation-inducing supplements (1 mM dexamethasone, 0.5 mM isobutylmethylxanthine (IBMX), 50 µM indomethacin), 1 % penicillin-streptomycin and 10 % FBS. The medium was refreshed every two days. At the end of 21 days, the coverslips were removed from the culture medium, washed three times with PBS and fixed with the fixative included in the staining kit. Intracellular lipid droplets indicating adipogenic differentiation were confirmed by Oil Red O staining (Karaoz et al., 2009).

2.3.2.3. Chondrogenic differentiation. After passage 3, eMSCs were cultured on a round glass coverslip using normal medium, with approximately 3×10^3 cells in 1 cm^2 of the culture dish. Afterwards, the cells were cultured in DMEM-F12 medium containing chondrogenic differentiation-inducing supplements (1 % Insulin-Transferin-Selenium (ITS), 100 nM dexamethasone, 0.1 mM ascorbate-2-phosphate, 1 mM sodium pyruvate and 10 ng/ml TGF-β) and 1 % penicillin-streptomycin. At the end of the 30th day, coverslips were removed from the culture medium, washed three times with PBS and fixed with the fixative included in the staining kit. At the end of 30th day, to detect chondrogenic differentiation of cells, Alcian blue staining was performed (Karaoz et al., 2009).

2.3.3. Proteomics Analysis

Proteomics analysis was performed on isolated eMSCs belonging to control, eutopic and ectopic endometrium groups to identify proteins affected by ER stress in more detail. Briefly, the cell free extracts were obtained, and the sample pools were constituted for further analyses. The protein extracts quality and quantity were verified by SDS-PAGE analyses. The peptide samples were prepared, and nLC-MS/MS analyses were performed (Okcu et al., 2023). The regulated ER proteins were determined and then applied for WB analyses.

2.3.3.1. Protein extraction and preparation of pooled samples. eMSC pellets from triplicate samples were washed with ice-cold PBS, suspended in RIPA lysis buffer and lysed using a bead beater with 0.2 mm stainless steel beads (Next Advance, USA). Supernatant containing soluble proteins were clarified and obtained after centrifugation. Protein concentrations were measured using Bradford protein assay (Bio-Rad, USA). For protein pool preparation, equal amount of protein from each sample was combined into a single clean tube and protein concentration was re-measured and an SDS-PAGE analyse were performed to evaluate the protein qualities of samples.

2.3.3.2. Protein digestion. Filter aided sample preparation (FASP) kit was used for preparation of peptide sample pools as recommended by the manufacturer (Abcam, USA). Briefly, 200 µg of proteins were mixed with 300 µl of 8 M urea and the mixtures were loaded onto a FASP spin columns and centrifuged at 15.000xg for 15 minutes. The flow through was discarded and the proteins were washed twice with 200 µL of 8 M urea. Then 100 µL of 50 mM iodoacetamide prepared in 8 M urea was added on top of the spin columns and vortexed briefly. The samples were then incubated at room temperature in the dark for 20 minutes. After incubation, the samples were centrifuged at 15.000 x g for 15 minutes and washed twice with 200 µL of 8 M urea and twice with 200 µl of 50 mM ammonium bicarbonate. For digestion, 0.5 µg trypsin in 40 µL of 50 mM ammonium bicarbonate solution was added to the FASP spin columns. The spin columns were briefly vortexed and incubated overnight at 37°C. Subsequently, the spin columns were placed into a new clean collection tube and 40 µl of 50 mM ammonium bicarbonate solution was used for washing of the spin columns and the peptides were eluted with 50 µl of 500 mM NaCl and concentrated with a vacuum concentrator. The peptides were resuspended in 0,1 % formic acid and peptide concentrations were measured by Qubit assay (Invitrogen, Q33211).

2.3.3.3. Liquid chromatography (LC)-tandem MS/MS analysis. The LC–MS/MS analysis was performed by using an Ultimate 3000 RSLC nanosystem (Thermo Fisher Scientific, USA) coupled to a Q Exactive mass spectrometer (Thermo Fisher Scientific, USA) equipped with an electrospray ion source. Briefly, the 500 ng peptides were separated on a C18 reversed-phase analytical column (2 µm, 75um×250 mm Thermo Scientific) using mobile phases A: 0.1 % formic acid and B: 0.1 % formic acid, 20 % acetonitrile at a flow rate of 300 nL/min. The chromatographic separation of the peptides started at 5 % of phase B (ACN with 0.1 % FA) for 10 minutes and gradually increased to 32 % in 185 min. The gradient performed from 32 % to 50 % of phase B in the next 20 min. Then phase B was increased in 15 minutes from 50 % to 90 %. The phase B was kept at 90 % for 10 minutes. The data-dependent acquisition was carried out with an MS scan mass window set at 250–2000 *m/z*, and the top 10 precursor ions were selected for higher energy collisional dissociation (HCD) fragmentation. The full scans were performed with a resolution of 70,000, a target value of 3×10^6 ions and a maximum

injection time of 100 ms, spray voltage of 2.4 kV. The MS/MS scans were performed with a 17,500 resolution, a 1×10^6 target value and a 100 ms maximum injection time. Each sample was analysed in triplicate.

2.3.3.4. MS data analysis. Raw MS/MS fragmentation spectra were analysed with Proteome Discoverer 2.2 software and searched against UniProt Homo sapiens reference proteome database with all isoforms (Human reference proteome: UP000005640, Human ER protome: SL-0095). Following parameters were used for protein identification; peptide mass tolerance of 10 ppm, MS/MS mass tolerance of 0.2 Da, mass accuracy of 2 ppm, tolerant miscarriage 1, minimum peptide length of 6 amino acids, fixed modification: carbamidomethylation of cysteines, and variable modifications: protein N-terminal acetylation and methionine oxidation. LFQ and validation were performed with the Proteome Discoverer 2.2 (Thermo Scientific, USA) that the workflow used to generate the intensity-based quantitation data (Sarihan et al., 2024). The target false discovery rate (FDR) threshold (strict) was set as 0.01 and target FDR (relaxed) was set as 0.05 using the Percolator node. A fold change of more than 5 and less than 0.2 was considered significant in terms of fold increase or decrease in proteins.

2.3.4. Western blot analysis

The pooled proteins were used for WB to validate the results of proteins levels by LC-MS/MS. For this, 30 µg protein sample was mixed with 6x laemmli sample buffer and loaded to 12 % SDS-PAGE gels. The gels were run and transferred onto nitrocellulose membranes and to prevent nonspecific bindings, the membranes were blocked for 1 h at room temperature in 5 % nonfat dried milk in TBS-T (%0.1 Tween 20, 50 mM Tris, 150 mM NaCl, pH 7.6). After blocking, the membranes were incubated overnight at +4°C with appropriately diluted polyclonal primary antibodies in TBS-T against GRP78 (1:500, SantaCruz, sc376768), TMED2 (1: 500, NBP1–80963, Novus Biologicals), DDRGK1 (1: 2000, 21445–1-AP, Proteintech), ERp44 (1: 1000, 16016–1-AP, Proteintech), RTN3 (1: 400, 12055–2-AP, Proteintech), and β-actin (1:2000, Bio-Rad). β-actin was used for normalization of each protein sample to ensure equal protein loading. Following three washes with TBS-T, the membranes were incubated with the secondary anti-mouse IgG-HRP antibody (1:10000, 170–5047, Bio-Rad) or anti-rabbit IgG-HRP antibody (1:10000, E-AB-1003, Elabscience®) for 1 h at room temperature. Then the proteins were visualized with an ECL Plus Western blotting detection system (GE Healthcare). The bands were quantitated by using Quantity One 1D image analysis software (Bio-Rad USA).

2.3.5. Histochemical and immunofluorescence stainings

The endometrial and endometriotic tissue samples (n=27, for all groups) were dehydrated with graded series of ethanol baths and toluene, then embedded in paraffin blocks. 4–5 µm thick sections were stained with H&E to determine LMP (proliferative and secretory phases).

To evaluate the ER-stress-related protein expressions in cell and tissue samples, single or double immunofluorescence staining were performed, respectively. For double staining, SUSD2 which was considered as an eMSC marker sufficient alone (Gargett et al., 2016) was used to detect eMSCs in endometrial tissues and the ER-stress related proteins identified as a result of proteomics analysis was performed together with SUSD2. In cell sample staining, single staining of the same ER-stress related proteins were analysed.

Subsequent to deparaffinization and rehydration, heat-induced antigen-retrieval was performed on tissue sections. After this stage, the same steps were applied to *cell* and *tissue* samples. Following the protein block step, primary antibodies (SUSD2 mouse monoclonal antibody, NBP3–09108, Novus Biologicals, 1:600 dilution; TMEM33 rabbit polyclonal antibody, NBP3–17553, Novus Biologicals, 1:200 dilution; TMED2 rabbit polyclonal antibody, NBP1–80963, Novus Biologicals, 1:200 dilution; DDRGK1 rabbit polyclonal antibody, 21445–1-AP, Proteintech, 1:50 dilution; TXNDC4 rabbit polyclonal antibody, 16016–1-AP, Proteintech, 1:50 dilution; RTN3 rabbit polyclonal antibody; 120552-AP, Proteintech, 1:100 dilution; TMX3 mouse monoclonal antibody, sc515248, SantaCruz Biotechnology) was performed at +4°C overnight incubation. After washing with TBS-T for 3×5 min, samples were incubated with secondary antibodies (ab150113 goat-anti mouse IgG H&L, Alexa Fluor 488®, Abcam, 1:600 dilution; ab150079, goat anti rabbit IgG H&L Alexa Fluor® 647, Abcam, 1:600 dilution) for 2 hours in the dark at room temperature and were covered with medium containing DAPI. Sections were examined on a laser scanning confocal microscope (Leica TCS SP8) with the LAS X (Leica Application Suite for Advanced Fluorescence) programme. In addition, staining intensities and localizations of related markers in photomicrographes were analyzed with ImageJ software (version 1.53e, NIH, USA).

2.3.6. RT-qPCR of eMSCs

As a result of proteomics analysis in eMSCs, ER-stress related proteins were identified whose translation was significantly changed compared to the control group. Then, the levels of genes encoding these proteins were analyzed by RT-qPCR. RNA isolation of eMSCs was performed using the Total RNA Isolation Kit according to the protocol provided by the manufacturer. RNA quantification (ng/µl) was read on a spectrophotometer at 260 nm. cDNA was synthesized using the Reverse Transcriptase kit to 2 µg of the total RNA amount and then these synthesized cDNAs were utilized in qRT-PCR analysis for each sample. Expression analysis of target genes was performed by RTq-PCR. GAPDH was used as a housekeeping gene.

2.3.7. Ultrastructural analysis of eMSCs

The 5×10^5 for each sample eMSCs were collected with trypsin/EDTA and centrifugated at 1000 rpm. 2.5 % glutaraldehyde was placed on the pelletized cells and fixed for 1 hour at +4ºC. At the end of primary fixation, glutaraldehyde was removed and cells were washed with Miloning buffer. Then, the cells were exposed to osmium tetroxide for 30 minutes at +4ºC for secondary fixation. Following this step, the fixed pellet was embedded in 2 % agar and divided into 1–2 mm^3 pieces and made ready for routine electron microscopic prossessing. eMSCs containing agars were dehydrated with ascending series of alcohols and treated with propylene oxide. Afterall, samples were embedded in araldite. 50–60 nm ultrathin sections were taken from the samples with an ultramicrotome. Sections taken on copper grids were contrasted with Reynolds lead citrate and uranyl acetate (Sezer et al., 2020). ER structures in the cell, mitochondria, apoptotic processes (vacuolization, presence of apoptotic bodies, nuclear bleb, degenerated mitochondria) and other organelles were analyzed utilization of transmission electron microscopy (Jeol-1011, Tokyo, Japan) (Roshangar et al., 2013).

2.3.8. Statistical Analysis

Statistical analyzes of the data were performed using SPSS 20.0 (SPSS, Chicago, USA) (Kiliç et al., 2023). Homogeneity of the variance and distribution of data were evaluated with the Kolmogorov-Smirnov test, and parametric or non-parametric tests were used according to the results. For normally distributed data, parametric one-way ANOVA test was used for multiple group analyses, and parametric t test was used for paired group analyses. Data that did not show normal distribution were analyzed with non-parametric tests: Kruskal Wallis test was used for multiple comparisons, and Mann-Whitney rank sum test was used for pairwise comparisons. Tests were performed within 95 % confidence interval and significant level was based on $p < 0.05$.

3. Results

3.1. Cell Samples

3.1.1. Isolation of eMSCs from Endometrial and Endometriotic Tissues

eMSCs were isolated from endometrial (control and eutopic) and endometriotic (ectopic) tissue samples at proliferative and secretory phases. They showed spindle, thin and long cell morphology, which is characteristic of mesenchymal stem cells (Fig. 1 A). At passage 3, cells were taken into flow cytometry analysis for characterization.

3.1.1.1. Flow Cytometry Analysis of eMSCs. In all groups, immunophenotypic characterizations of eMSCs at passage 3 were performed by flow cytometry analysis. Cells in the population were negative for endothelial and hematopoietic markers (CD31, CD34, CD45 and HLA-DR) and positive for eMSC markers (CD29, CD44, CD73, CD90, CD105, CD140b and CD146) (Fig. 1 C).

3.1.1.2. eMSCs Differentiation

3.1.1.2.1. Osteogenic Differentiation. For osteogenic differentiation, eMSCs were seperated into control and experimental groups: While the cells in the control group were given normal medium, the cells in the experimental group were given medium containing osteogenic differentiation supplements. At the end of the 28th day, calcium nodules in the experimental group samples were stained red with Alizarin Red S (Fig. 1B).

3.1.1.2.2. Adipogenic Differentiation. For adipogenic differentiation, eMSCs were seperated into control and experimental groups: While cells in the control group were given normal medium, cells in the experimental group were given medium containing adipogenic differentiation supplements. At the end of the 21st day, lipid droplets in the experimental group were stained red with Oil Red O (Fig. 1B).

3.1.1.2.3. Chondrogenic Differentiation. For chondrogenic differentiation, eMSCs were seperated into control and experimental groups. While the cells in the control group were given normal medium, the cells in the experimental group were given medium containing chondrogenic differentiation supplements. At the end of the 30th day, in the experimental group, chondrogenic extracellular matrix of experimental group was stained bluish-green with Alcian blue (Fig. 1B).

3.1.1.3. Proteomics Analysis of eMSCs. Proteomics analysis was performed in order to examine the proteins whose amount changes related to ER stress in eMSCs, in more detail and comprehensively.

3.1.1.4. SDS-PAGE Analysis. In all groups, SDS-PAGE analysis was performed to evaluate the quality of proteins isolated from eMSCs. For this purpose, equal amounts of protein were loaded into the wells and run in the gel. The band quality and quantity were found to be suitable for further analysis (Fig. 2 A).

3.1.1.5. LC-MS/MS Analysis. Peptide concentrations of proteins prepared for mass spectrometry with the FASP protocol were measured after tryptic cutting. Peptides were separated and sent to the Thermo Q-exactive brand mass spectrometer, and data-dependent data collection was carried out on this device. Unpaired and singly charged ions were removed from the MS/MS analysis and dynamic exclusion was performed automatically. As a result of LC-MS/MS analysis, raw data were analyzed with Proteome Discoverer 2.2 (Thermo Scientific, USA) for protein identification. All samples were grouped separately based on Principal Component Analysis (PCA) analysis (Fig. 2B-C). The minimum number of peptides identified for each protein was considered to be two and the data were searched against organism specific data available in the UniProt/SwissProte database. Since the proteome data contains a lot of data and the hypothesis is about ER stress in eMSCs, ER proteome analysis was focused more on.

As a result of the label-free quantification method using the data obtained as a result of LC-MS/MS analysis of proteins, increases and decreases in the proteins in the experimental groups were detected compared to the control group. A fold change of more than 5 and less than 0.2 was considered significant in terms of fold increase or decrease

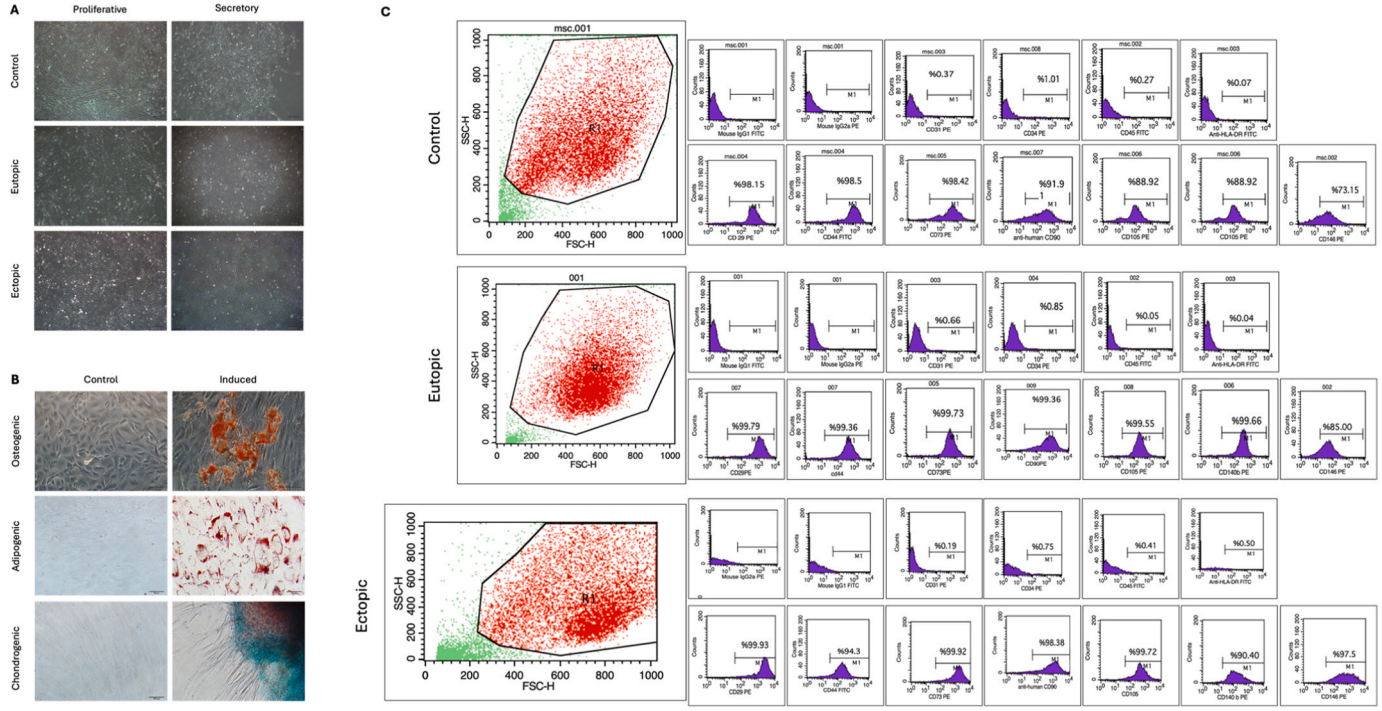


Fig. 1. (A) eMSCs isolated from control, eutopic and ectopic samples at proliferative and secretory phases. Scale bar: 200 μm. **(B)** Alizarin Red S, Oil Red O, and Alcian blue staining show osteogenic, adipogenic and chondrogenic differentiation of eMSCs, respectively. Scale bar: 50 μm **(C)** Characterization of eMSCs belonging to control, eutopic and ectopic endometrium groups by flow cytometry.

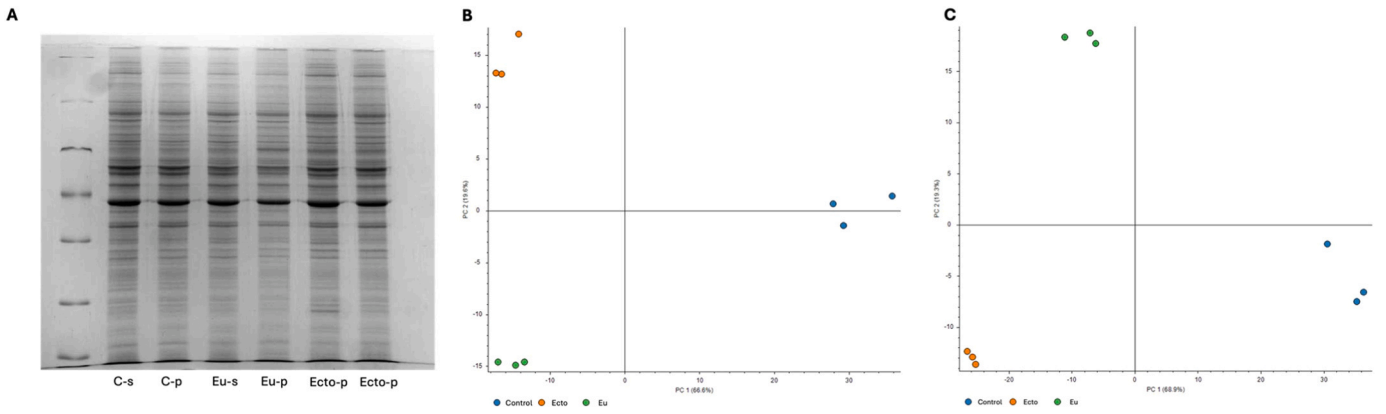


Fig. 2. (A) SDS-PAGE Analysis of protein extracts belonging to all groups. **(B and C)** Principal Component Analysis (PCA) analysis of protein expression profiles obtained from nLC-MS/MS analyses belonging to proliferative and secretory phases, respectively. As a result of the analysis obtained; the readings of control, eutopic and ectopic samples were clustered into 3 different groups. *C-s: Control-secretory, C-p: Control-proliferative, Eu-s: Eutopic-secretory, Eu-p: Eutopic-proliferative, Ecto-s: Ectopic-secretory, Ecto-p: Ectopic-proliferative.*

in proteins. In subsequent analysis, it was determined that 6 proteins related to the ER stress pathway (ERp44, RTN3, TMED2, TMEM33, TMX3, DDRGK1) showed significant differences compared to the control group (Supplementary Figure 1–2, Fig. 3).

When ER stress-related proteins that showed significant differences between the control and eutopic endometrium groups of the proliferative phase were examined; ERp44, TMED2 and RTN3 increased whereas TMX3 and TMEM33 decreased in eutopic endometrium group. When the control and ectopic endometrium groups were compared, TMED2 and RTN3 increased while TMX3 decreased in the ectopic endometrium. When eutopic and ectopic endometrium groups were compared, ERp44 increased whereas RTN3 and TMEM33 decreased in eutopic endometrium (Fig. 3).

When the ER stress-related proteins of control, eutopic and ectopic endometrium groups of the secretory phase were examined; it was determined that DDRGK1 protein level significantly decreased in the eutopic and ectopic endometrium groups compared to the control group (Fig. 3). However, according to LC-MS/MS analysis, there were no

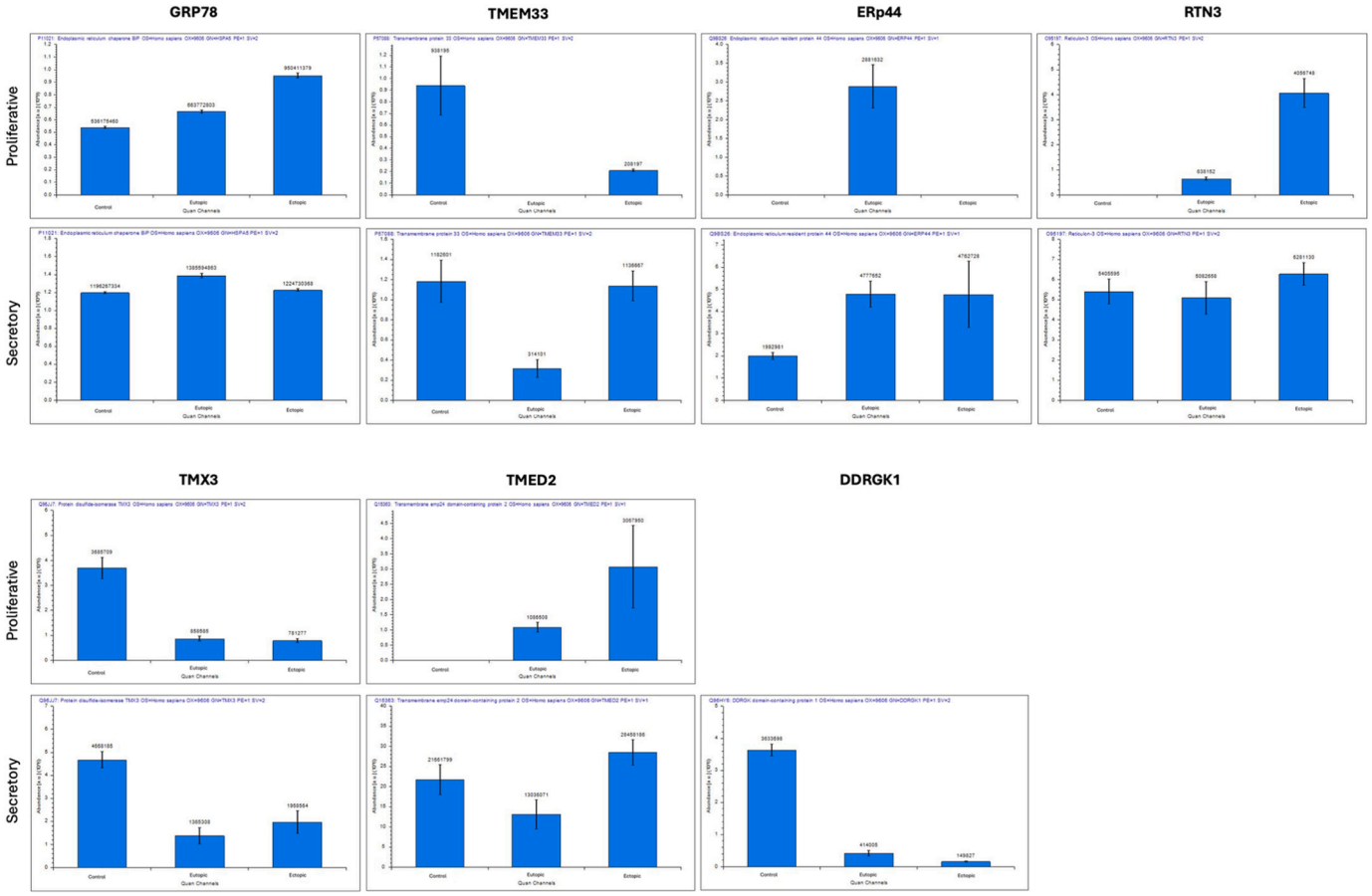


Fig. 3. As a result of nLC-MS/MS (ER proteome) analyses, GRP78, TMEM33, ERp44, RTN3, TMX3, TMED2 and DDRGK1 protein concentrations in control, eutopic and ectopic endometrium groups at the proliferative and secretory phases (DDRGK1 protein were not identified in proliferative phase).

siginificant difference between groups except for DDRGK1 protein levels.

3.1.1.6. Western Blot and Immunofluorescence Analysis of eMSCs. WB and IF analysis of 6 proteins identified as a result of proteomics analysis and GRP78, one of the most known ER stress chaperone markers, was performed.

3.1.1.6.1. GRP78. When GRP78 expression of eMSCs was examined in control, eutopic and ectopic endometrium groups belonging to the proliferative and secretory phases (Fig. 4 A); increased GRP78 expression was observed in the eutopic and ectopic endometrium groups compared to the control group, however no statistically significant difference was found between the groups. (Fig. 4B-C).

When the protein bands of GRP78 were evaluated; although GRP78 expression levels were increased in the ectopic endometrium groups of the proliferative and secretory stages compared to their own controls, there was no statistically significant difference between the groups. (Fig. 4D-F).

3.1.1.7. TMEM33. When the control, eutopic and ectopic endometrium groups of the proliferative phase were compared (Fig. 5 A); it was determined that TMEM33 expression in eMSCs isolated from ectopic endometrium showed a statistically significant increase compared to that in those isolated from control and eutopic endometrium ($p < 0.001$). Also, TMEM33 expression was significantly higher in the eutopic endometrium group than in the control group ($p = 0.010$) (Fig. 5B). According to LC-MS/MS analysis, although TMEM33 expression level were decreased in eutopic group in secretory phase, there were no statistically significant difference among groups.

3.1.1.8. ERp44. When the control, eutopic and ectopic endometrium groups of the proliferative phase were examined (Fig. 6 A); ERp44 expression statistically decreased in ectopic endometrium group compared to the eutopic endometrium group ($p < 0.001$) (Fig. 6B).

As a result of the ratio of ERp44 protein bands to β-actin bands; it was determined that the amount of ERp44 protein significantly decreased in the eutopic and ectopic endometrium groups of the proliferative phase compared to the control group ($p = 0.001$ and $p = 0.006$). In the western blot analysis, at the secretory phase, ERp44 protein level were significantly increased in eutopic and ectopic endometrium groups compared to control group (control-eutopic $p < 0.001$; control-ectopic $p = 0.039$). Also, expression level of this protein were higher in eutopic endometrium group than in ectopic group (eutopic-ectopic $p = 0.007$) (Fig. 6C-E).

3.1.1.9. RTN3. When the control, eutopic and ectopic endometrium groups of the proliferative phase were examined (Fig. 7 A); it was determined that RTN3 expression in eMSCs isolated from ectopic endometrium showed a statistically significant increase compared to eMSCs isolated from the eutopic group ($p < 0.001$) (Fig. 7B).

As a result of the ratio of protein bands of RTN3 to β-actin bands; It was determined that the amount of RTN3 protein significantly increased in the ectopic endometrium group of the proliferative phase compared to the control and eutopic endometrium groups ($p < 0.001$). No statistically significant difference was observed between control, eutopic and ectopic endometrium groups at the secretory phase (Fig. 7C-E).

3.1.1.10. TMX3. When TMX3 expression of eMSCs was examined in control, eutopic and ectopic endometrium groups belonging to the proliferative phase (Fig. 8 A); decreased TMX3 expression was observed in the ectopic endometrium group compared to the control group. (Fig. 8B).

As a result of the ratio of protein bands of TMX3 to β-actin bands; It was determined that the amount of TMX3 protein significantly decreased in the eutopic and ectopic endometrium groups at the proliferative phase when compared to the control group ($p < 0.001$) (Fig. 8C-D)

3.1.1.11. TMED2. When the control, eutopic and ectopic endometrium groups of the proliferative phase were compared (Fig. 9 A); it was

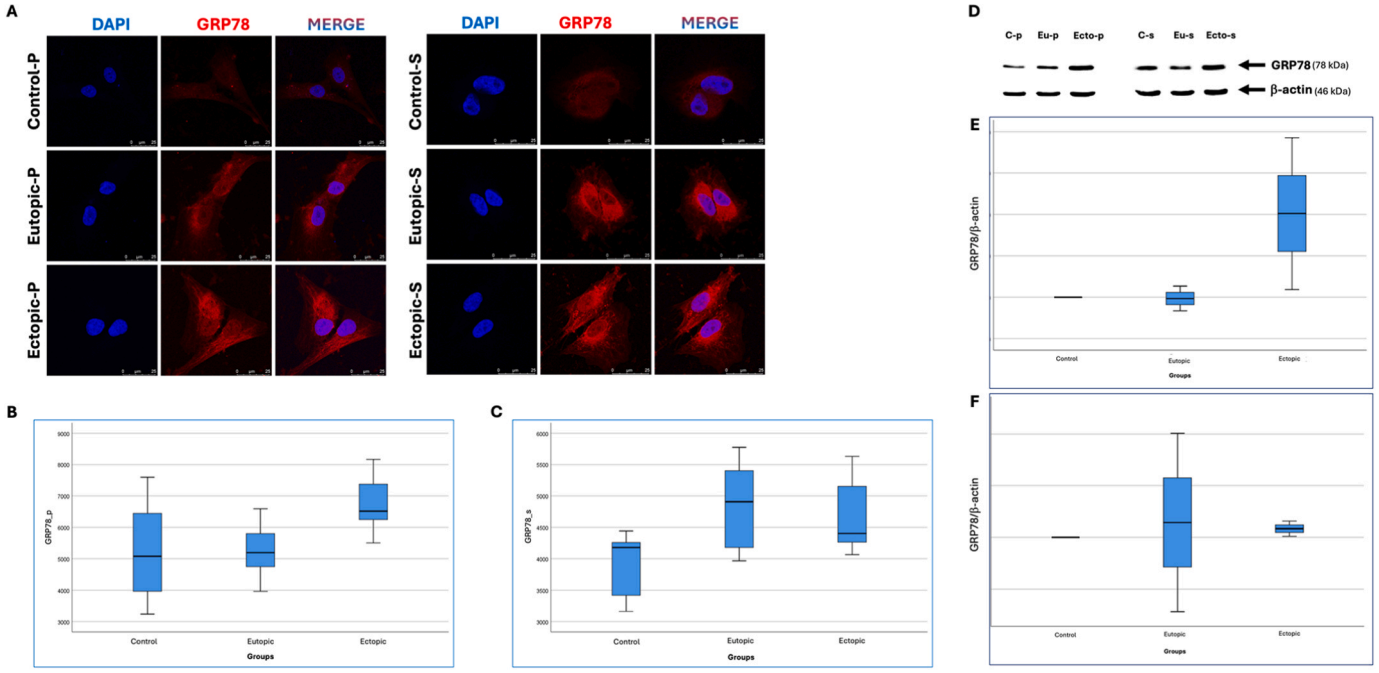


Fig. 4. (A) IF staining of GRP78 in eMSCs belonging to the proliferative and secretory phases. Size bar: 25 μm. Negative control was inserted in the right upper side (white frame). GRP78 expression level in control, eutopic and ectopic endometrium groups at proliferative **(B)** and secretory **(C)** phases. **(D)** GRP78 and β-actin bands belonging to all groups. **(E)** GRP78 protein amount in control, eutopic and ectopic endometrium groups of the proliferative phase. **(F)** GRP78 protein amount in control, eutopic and ectopic endometrium groups of the secretory phase. *C-s: Control-secretory, C-p: Control-proliferative, Eu-s: Eutopic-secretory, Eu-p: Eutopic-proliferative, Ecto-s: Ectopic-secretory, Ecto-p: Ectopic-proliferative.*

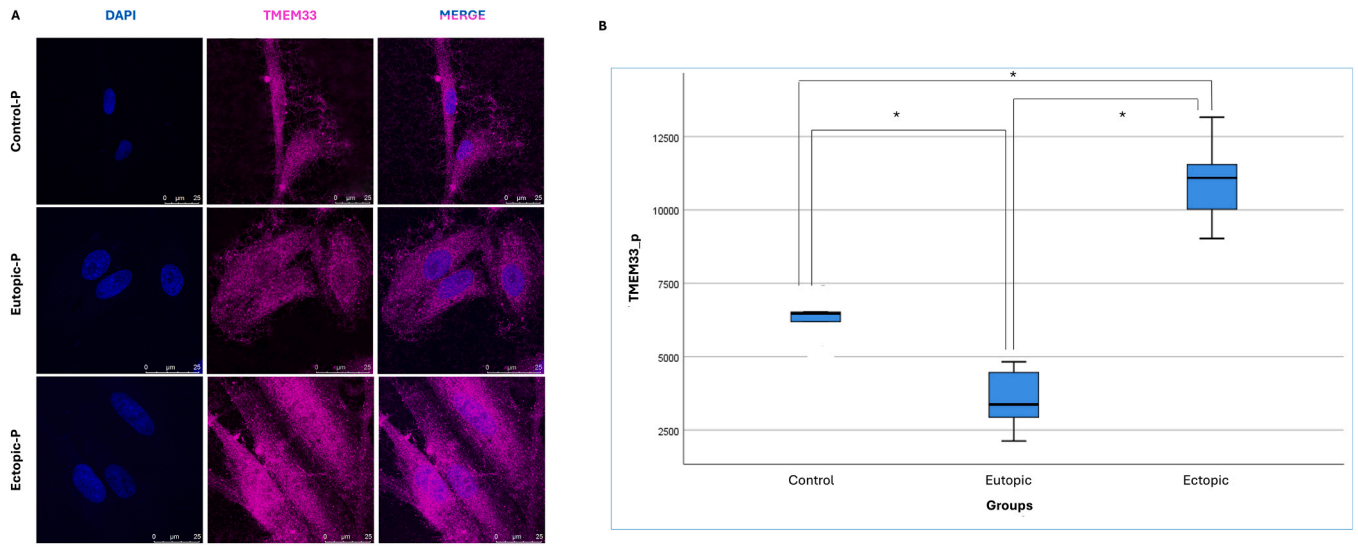


Fig. 5. **(A)** IF staining of TMEM33 in eMSCs belonging to the proliferative phase. Size bar: 25 μm. Negative control was inserted in the right upper side (white frame). **(B)** TMEM33 expression level in control, eutopic and ectopic endometrium groups at proliferative phase.

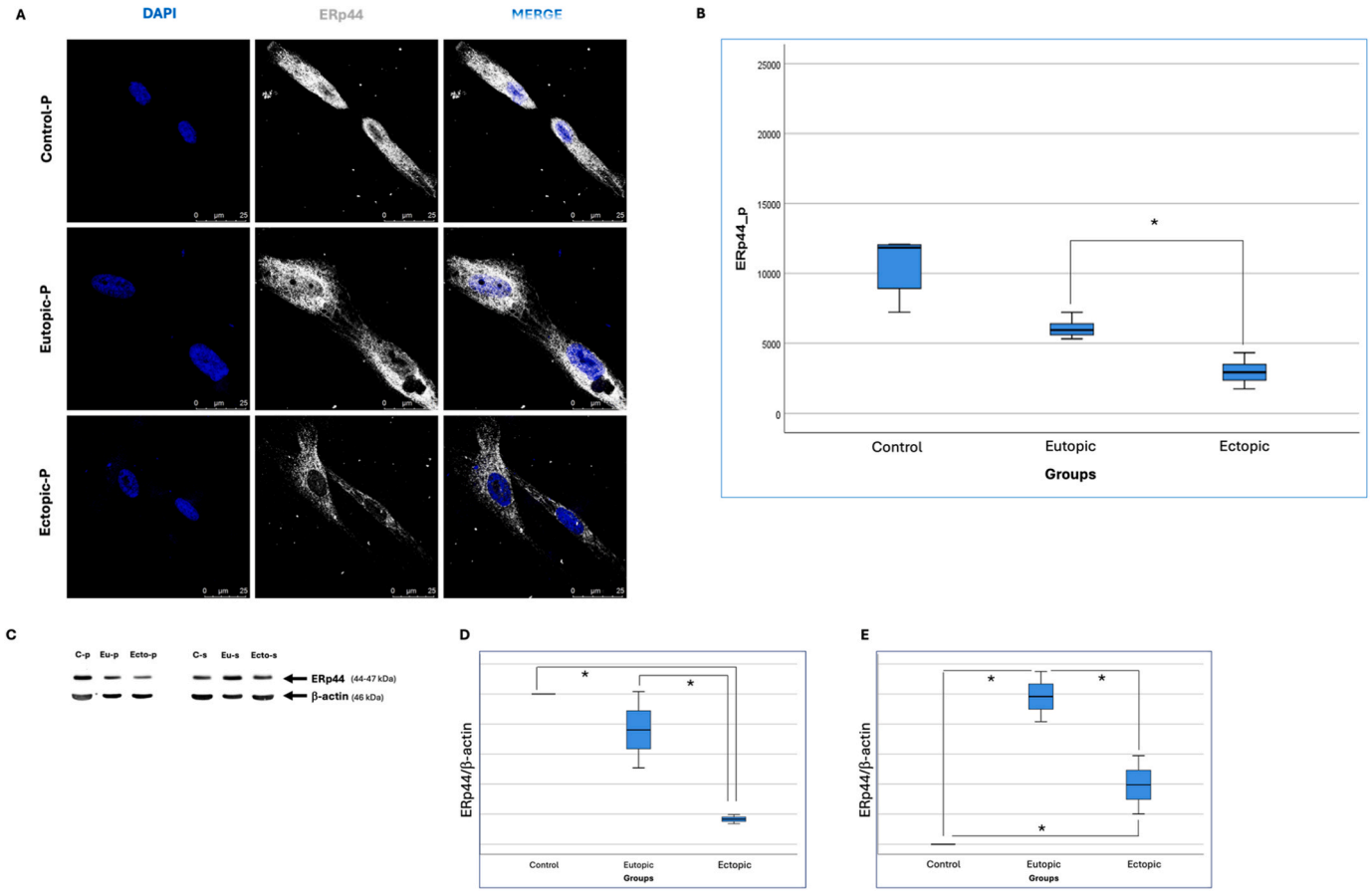


Fig. 6. **(A)** IF staining of ERp44 in eMSCs belonging to the proliferative phase. Size bar: 25 μm. Negative control was inserted in the right upper side (white frame). **(B)** ERp44 expression level in control, eutopic and ectopic endometrium groups at proliferative phase. **(C)** ERp44 and β-actin bands belonging to all groups. **(D)** ERp44 protein amount in control, eutopic and ectopic endometrium groups of the proliferative phase. **(E)** ERp44 protein amount in control, eutopic and ectopic endometrium groups of the secretory phase. *C-s: Control-secretory, C-p: Control-proliferative, Eu-s: Eutopic-secretory, Eu-p: Eutopic-proliferative, Ecto-s: Ectopic-secretory, Ecto-p: Ectopic-proliferative.*

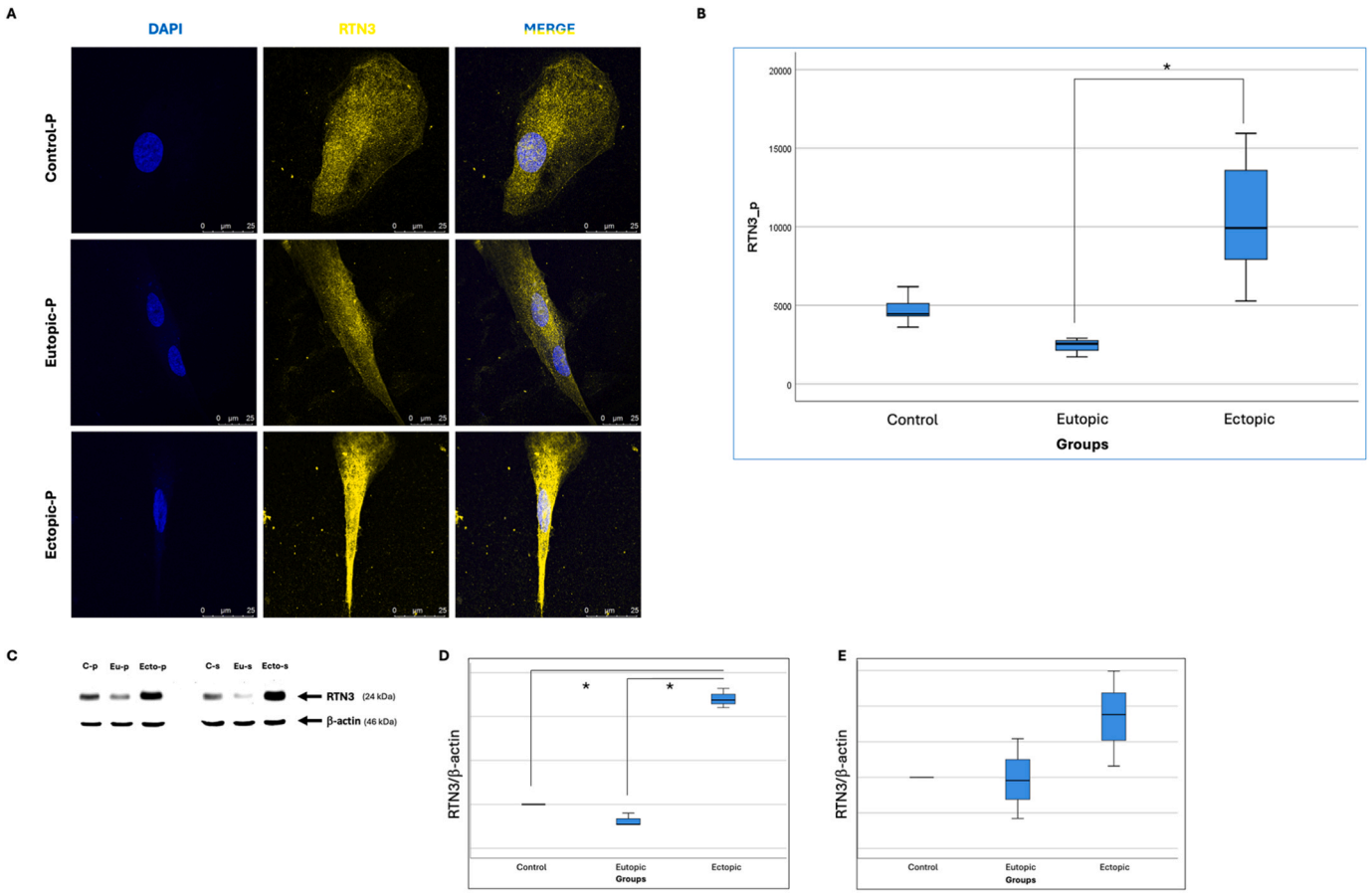


Fig. 7. **(A)** IF staining of RTN3 in eMSCs belonging to the proliferative phase. Size bar: 25 μm. Negative control was inserted in the right upper side (white frame). **(B)** RTN3 expression level in control, eutopic and ectopic endometrium groups at proliferative phase. **(C)** RTN3 and β-actin bands belonging to all groups. **(D)** RTN3 protein amount in control, eutopic and ectopic endometrium groups of the proliferative phase. **(E)** RTN3 protein amount in control, eutopic and ectopic endometrium groups of the secretory phase. *C-s: Control-secretory, C-p: Control-proliferative, Eu-s: Eutopic-secretory, Eu-p: Eutopic-proliferative, Ecto-s: Ectopic-secretory, Ecto-p: Ectopic-proliferative.*

determined that TMED2 expression in eMSCs isolated from control and ectopic endometrium showed a statistically significant increase compared to those isolated from the eutopic group ($p = 0.018$ and $p = 0.004$) (Fig. 9B).

As a result of the ratio of protein bands of TMED2 to β-actin bands; it was determined that the amount of TMED2 protein significantly increased in the ectopic endometrium group of the proliferative phase than in the control and eutopic endometrium groups ($p = 0.004$ and $p = 0.008$) (Fig. 9C-E). No significant difference was found between control and eutopic endometrium. In the secretory phase, the amount of TMED2 decreased in the eutopic endometrium group and increased in the ectopic endometrium group when compared to the control group. However, these differences were not found to be statistically significant.

3.1.1.12. DDRGK1. When the control, eutopic and ectopic endometrium groups of the secretory phase were compared (Fig. 10 A); it was determined that DDRGK1 expression was significantly decreased in the eutopic and ectopic endometrium group compared to the control group ($p < 0.001$) (Fig. 10B).

As a result of the ratio of protein bands of DDRGK1 to β-actin bands; it was determined that DDRGK1 expression significantly decreased in eutopic and ectopic endometrium groups belonging to both proliferative and secretory phases compared to their controls ($p = 0.006$ and $p = 0.004$; $p = 0.002$ and $p = 0.012$). There was no statistically significant difference between eutopic and ectopic endometrium groups (Fig. 10C-E).

3.1.2. RT-qPCR Analysis of eMSCs

In RT-qPCR analysis of eMSCs; GRP78, the best-known ER chaperone protein; three main proteins of the UPR pathway, IRE1a, PERK and ATF6; and 6 proteins determined as a result of proteomics analysis (DDRGK1, RTN3, ERp44, TMED2, TMEM33, TMX3) were analyzed at the gene level.

When the gene expression analysis of eMSCs in control, eutopic and ectopic endometrium of the proliferative phase was performed; GRP78, DDRGK1, RTN3 and IRE1a gene expression in the ectopic endometrium group showed a significant increase compared to the control and eutopic endometrium. When the control and eutopic endometrium groups were evaluated among themselves; only DDRGK1 showed a significant increase in eutopic endometrium compared to the control group (Fig. 11A).

In the gene expression analysis of eMSCs in control, eutopic and ectopic endometrium groups belonging to the proliferative phase; ERp44 was significantly reduced in eutopic endometrium compared to the control group whereas PERK expression increased and ERp44 expression decreased in ectopic endometrium. When eutopic and ectopic endometrium groups are compared within themselves; all genes except ATF6 showed a statistically significant increase compared to the eutopic endometrium group (Fig. 11A).

When gene expression analysis of eMSCs in the control, eutopic and ectopic endometrium groups of the secretory phase was performed; DDRGK1 and IRE1a gene expression levels in the ectopic endometrium group showed a significant increase compared to the control group (Fig. 11B).

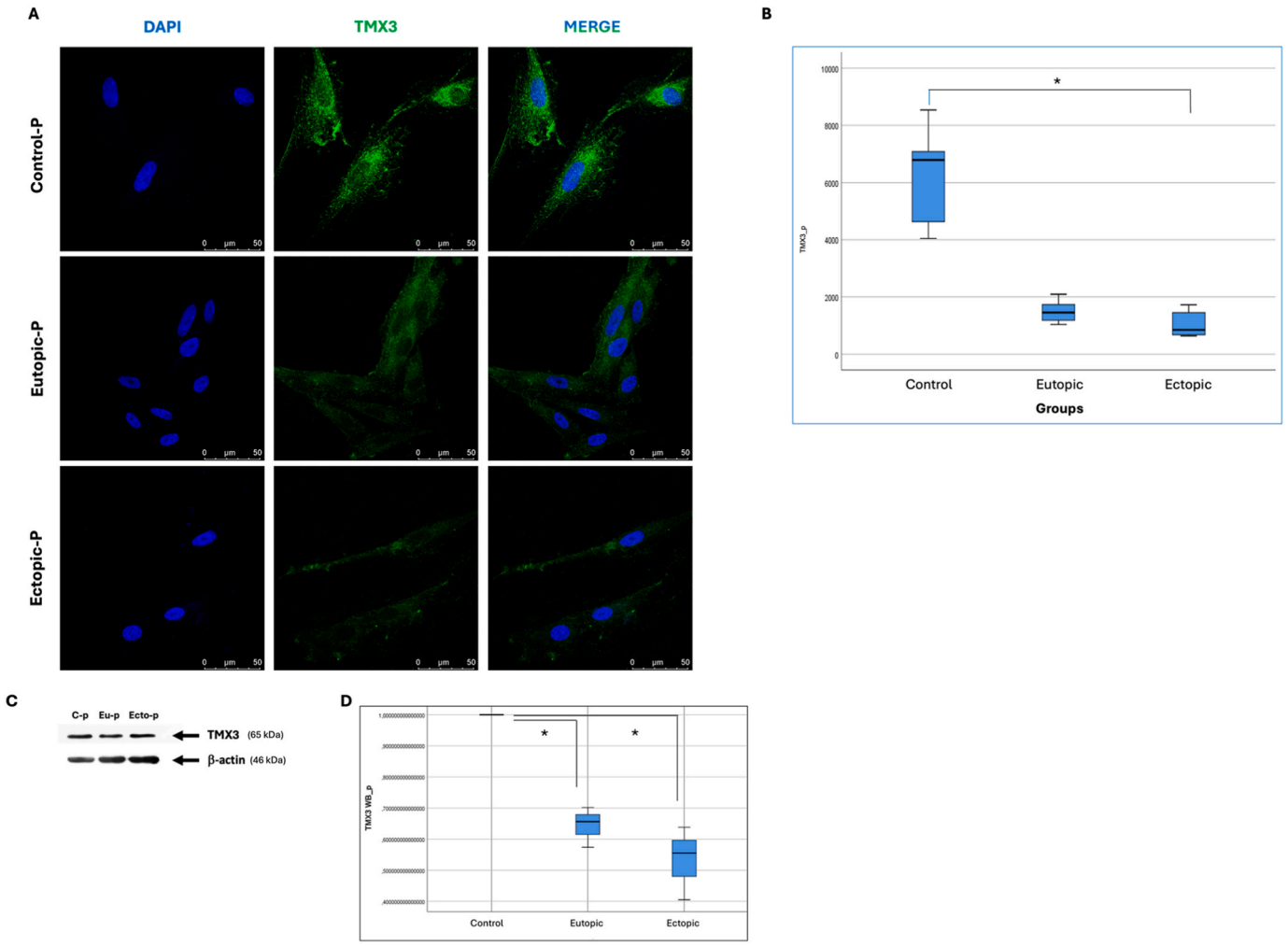


Fig. 8. **(A)** IF staining of TMX3 in eMSCs belonging to the proliferative phase. Size bar: 25 μm. Negative control was inserted in the right lower side (white frame). **(B)** TMX3 expression level in control, eutopic and ectopic endometrium groups at proliferative phase. **(C)** TMX3 and β-actin bands belonging to all groups in proliferative phase. **(D)** TMX3 protein amount in control, eutopic and ectopic endometrium groups of the proliferative phase. *C-p: Control-proliferative, Eu-p: Eutopic-proliferative, Ecto-p: Ectopic-proliferative.*

When gene expression analysis of eMSCs in the control, eutopic and ectopic endometrium groups of the secretory phase was performed; PERK expression in the ectopic endometrium group showed a significant increase compared to both the control and eutopic endometrium groups. PERK gene expression in the eutopic endometrium group also showed a statistically significant increase compared to the control group. TMEM33 gene expression level showed a significant increase in the ectopic endometrium group compared to the control group (Fig. 11B).

3.1.3. Ultrastructural Analysis of eMSCs

When the eMSCs belonging to control group at the proliferative phase were examined from an ultrastructural perspective; gER and Golgi apparatus with normal morphology and healthy mitochondria were observed (Fig. 12A-D). When the control group eMSCs of the secretory phase are examined; healthy mitochondria and secretory vesicles with gER and Golgi apparatus showing normal morphology were observed (Fig. 12E-H). In addition to secretory vesicles, exocytotic vesicle (Fig. 12F) and sER structures (Fig. 12H) were also observed.

When eMSCs belonging to eutopic endometrium group at proliferative phase were examined; autophagosome structures containing gER, elongated mitochondria, late autolysosomes and enlarged Golgi vesicles were observed (Fig. 13A-E). When the eMSCs belonging to eutopic endometrium group at the secretory phase were examined; enlarged gER vesicles/lumen, apoptotic bodies containing enlarged gER, excessive amounts of lysosomes and autolysosome structures were observed (Figure13 F-J).

When eMSCs belonging to ectopic group at the proliferative phase were examined; apoptotic bodies containing enlarged gER vesicles, enlarged gER lumen, mitochondria with disrupted crista structure, autolysosome and autophagolysosome structures and multivesicular bodies were observed (Fig. 14A-D). When the eMSCs belonging to ectopic endometrium group at the secretory phase were examined; excessive amounts of lysosome structures, enlarged gER vesicles, autophagosome and autolysosome structures were observed (Figure14 E-H).

3.1.4. Tissue Samples

3.1.4.1. Hematoxylin & Eosin (H&E) Staining. The phase of the menstrual cycle belonging to all groups was determined by H&E sections as well as the declaration of the Obstetrician and the patient. In H&E sections at the proliferative phase, endometrial gland and epithelial structures were seen. The round or tubular type of the glands and the intact appearance of the stroma comfirmed that the sample belonged to the proliferative phase (Fig. 15A-C). In H&E sections at the secretory phase, endometrial gland and epithelial structures were seen. Presence of corkscrew-shaped folded gland structures and edematous stroma comfirmed that the sample belonged to the secretory phase (Fig. 15D-F). When H&E sections of endometriotic samples belonging to the ectopic

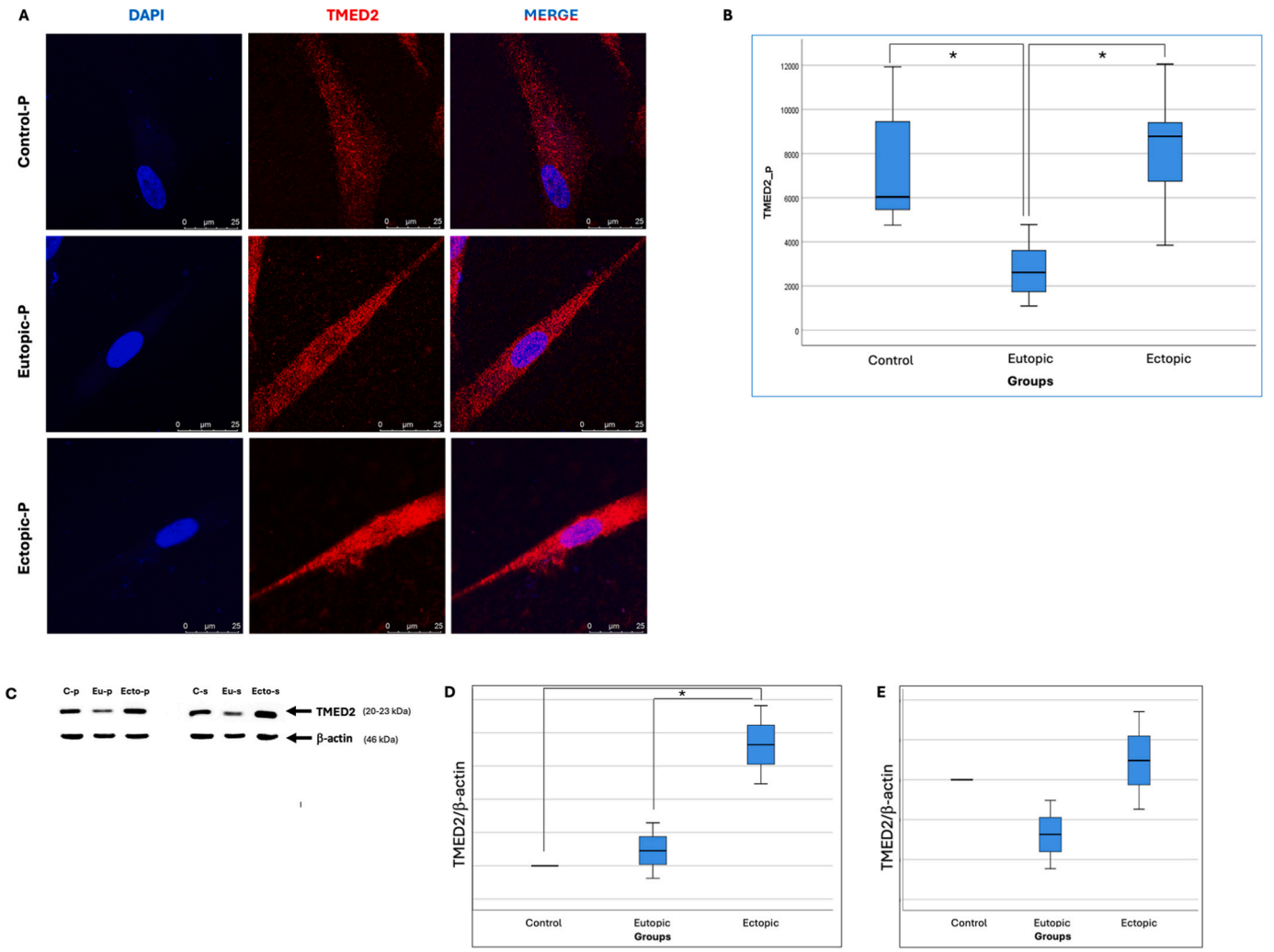


Fig. 9. **(A)** IF staining of TMED2 in eMSCs belonging to the proliferative phase. Size bar: 25 μm. Negative control was inserted in the right upper side (white frame). **(B)** TMED2 expression level in control, eutopic and ectopic endometrium groups at proliferative phase. **(C)** TMED2 and β-actin bands belonging to all groups. **(D)** TMED2 protein amount in control, eutopic and ectopic endometrium groups of the proliferative phase. **(E)** TMED2 protein amount in control, eutopic and ectopic endometrium groups of the secretory phase. *C-s: Control-secretory, C-p: Control-proliferative, Eu-s: Eutopic-secretory, Eu-p: Eutopic-proliferative, Ecto-s: Ectopic-secretory, Ecto-p: Ectopic-proliferative.*

group were examined; endometrium-like gland and stroma structures, epithelium surrounding the endometriotic cyst, hemorrhage and hemosiderin granules were observed (Fig. 15G-I).

3.1.5. Demonstration of ER Stress-related Proteins in Tissue eMSCs by Immunofluorescence Method

In addition to the expression analysis of ER-stress-related markers in eMSCs isolated from control, eutopic and ectopic endometrium groups, the expression of these markers in eMSCs directly in tissue was also evaluated. Fort his purpose, double staining of the 6 proteins together with SUSD2, which is accepted as a single eMSC marker, were performed.

3.1.5.1. SUSD2-TMEM33 Immunofluorescence Analysis. When TMEM33 expression in the proliferative and secretory phases was evaluated; there was a decrease in the eutopic endometrium group and an increase in the ectopic endometrium group compared to the control group (Fig. 16).

3.1.5.2. SUSD2-ERp44 Immunofluorescence Analysis. At the proliferative phase, ERp44 expression decreased in eutopic and ectopic endometrium group compared to the control group. At the secretory phase, ERp44 expression increased in eutopic and ectopic endometrium group compared to the control group. ERp44 expression was also observed in endometrial glands in eutopic endometrial tissue (Fig. 17).

3.1.5.3. SUSD2-RTN3 Immunofluorescence Analysis. At the proliferative phase, RTN3 expression increased in ectopic endometrium group compared to the control and eutopic endometrium groups. Although RTN3 expression was lower in eMSCs of the eutopic endometrium, significant RTN3 expression in the endometrial glands was noted. In the secretory phase, RTN3 expression increased in control and ectopic endometrium groups compared to the eutopic endometrium group (Fig. 18).

3.1.5.4. SUSD2-TMED2 Immunofluorescence Analysis. At the proliferative phase, TMED2 expression increased in eutopic and ectopic endometrium groups compared to the control group. When TMED2 expression was examined in the groups belonging to the secretory phase, it was observed that TMED2 expression was higher in eMSCs in the ectopic endometrium group than in the eutopic endometrium group (Fig. 19).

3.1.5.5. SUSD2-DDRGK1 Immunofluorescence Analysis. At the proliferative phase, DDRGK1 level was significantly decreased in the eutopic

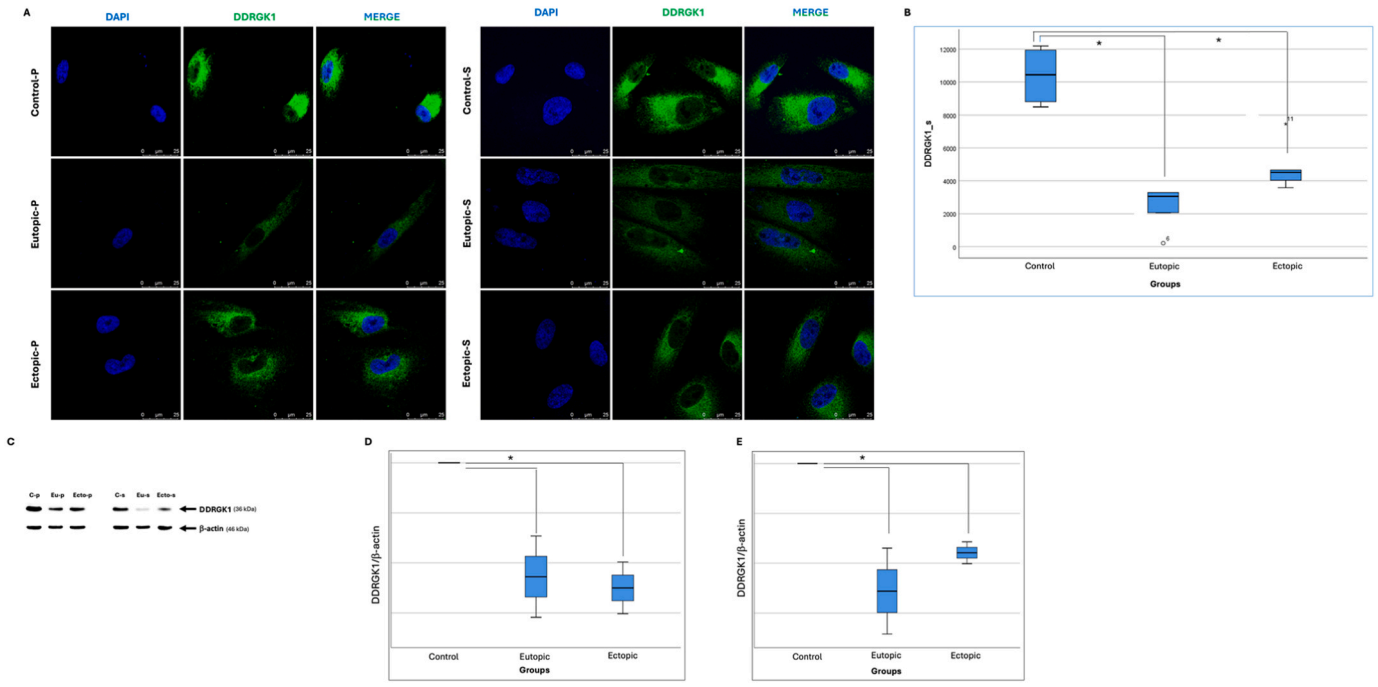


Fig. 10. **(A)** IF staining of DDRGK1 in eMSCs belonging to the proliferative and secretory phases. Size bar: 25 μm. Negative control was inserted in the right upper side (white frame). **(B)** DDRGK1 expression level in control, eutopic and ectopic endometrium groups at secretory phase. **(C)** DDRGK1 and β-actin bands belonging to all groups. **(D)** DDRGK1 protein amount in control, eutopic and ectopic endometrium groups of the proliferative phase. **(E)** DDRGK1 protein amount in control, eutopic and ectopic endometrium groups of the secretory phase. *C-s: Control-secretory, C-p: Control-proliferative, Eu-s: Eutopic-secretory, Eu-p: Eutopic-proliferative, Ecto-s: Ectopic-secretory, Ecto-p: Ectopic-proliferative.*

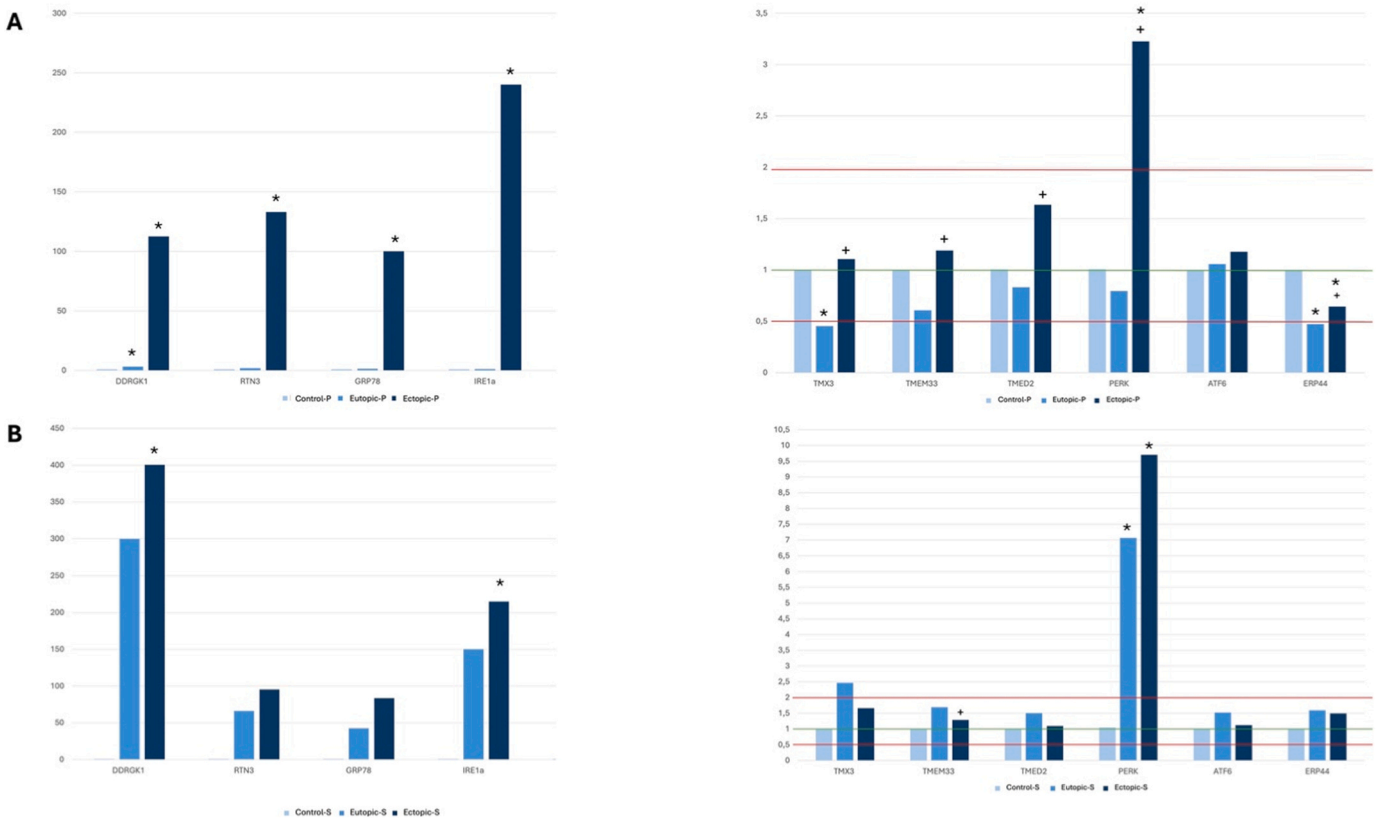


Fig. 11. DDRGK1, RTN3, GRP78, IRE1a, TMX3, TMEM33, TMED2, PERK, ATF6 and ERp44 gene expressions at the proliferative (A) and secretory (B) phases in control, eutopic and ectopic endometrium groups. *; represents significance at the $p < 0.05$ level when compared to control group. +; represents significance at the $p < 0.05$ level when compared to eutopic group.

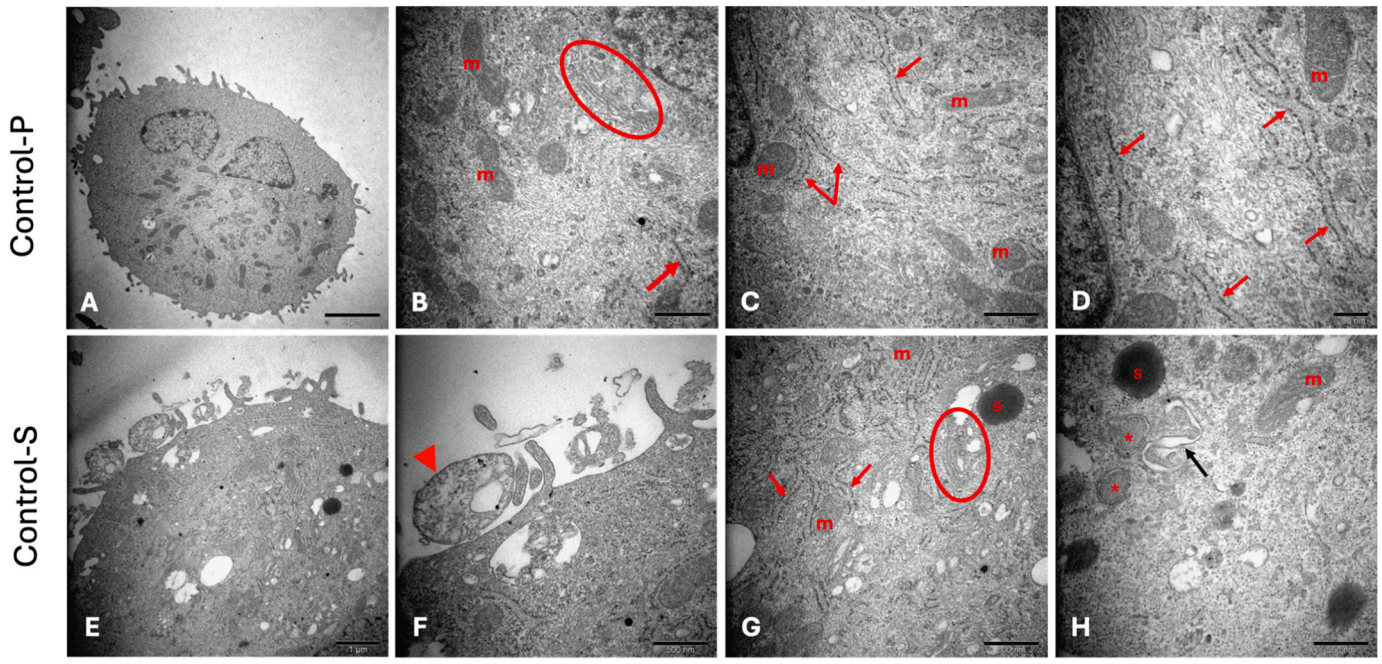


Fig. 12. Electron microscopic photomicrographs of the control eMSCs in proliferative **(A-D)** and secretory phases **(E-H)**. Red arrow: gER; red arrowhead: exocytosis; red star: double membrane autophagosome; black arrow: sER; m: mitochondrion, s: secretory vesicle. The area enclosed in the red circle shows the Golgi apparatus. Uranyl acetate and lead citrate. Scale bar: A: 2 μm; E: 1 μm; B, C, F, H: 500 nm; D, G: 200 μm.

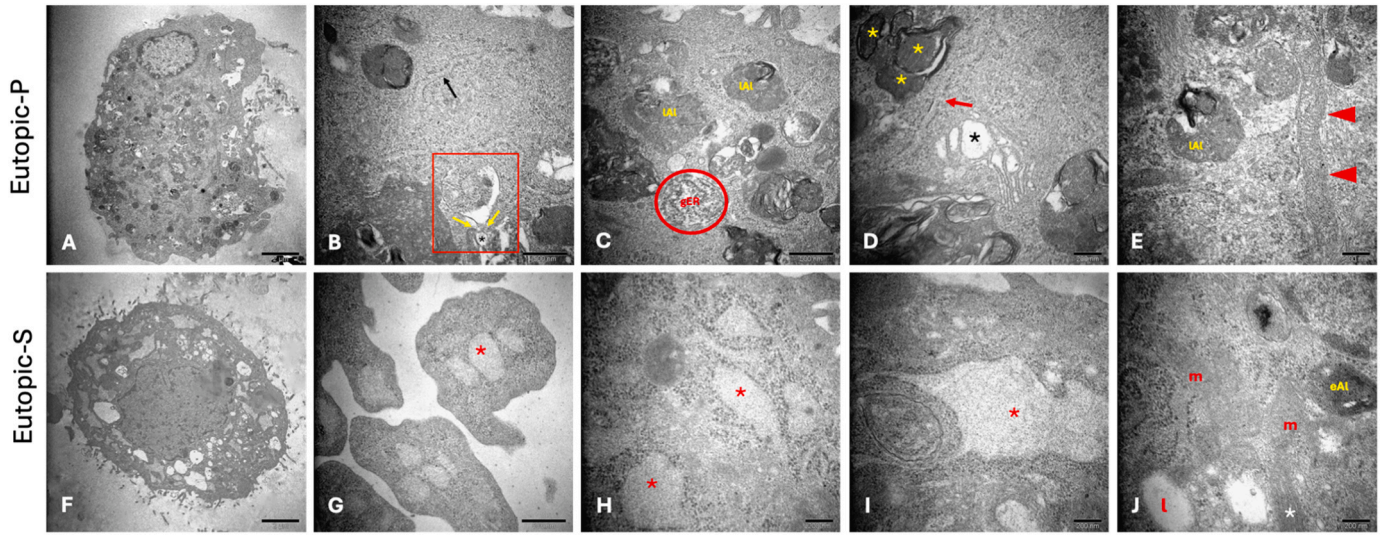


Fig. 13. Electron microscopic photomicrographs of the eutopic eMSCs in proliferative **(A-E)** and secretory phases **(F-J)**. Red arrow: gER; black arrow: sER; red star: enlarged ER sacs; black star: enlarged Golgi sacs; l: lysosome; eAl: early autolysosome; lAl: late autolysosome; yellow star: double membrane autolysosome; red frame: fusing of gER-containing autophagosome with lysosome (ERphagy); red circle: autolysosome containing gER; red arrowhead: elongated mitochondrion; m: mitochondrion. Uranyl acetate and lead citrate. Scale bar: A, F: 2 μm; B, C, G: 500 nm; D, I, J: 200 μm.

and ectopic endometrium groups compared to the control group. Similarly, it was determined that the expression of DDRGK1 in the secretory phase was significantly decreased in the eutopic and ectopic endometrium groups compared to the control group (Fig. 20).

4. Discussion

Endometriosis, defined as the presence of glands and stroma of the endometrium outside their normal location, is a common benign gynecological disease. It is most commonly found over the pelvic peritoneum; It is a hormone-dependent disease and is most common in women of reproductive age (Giudice and Kao, 2004).

Current approaches are not effective in the treatment of the disease, and the recurrence rate is approximately 50 % in the first 5 years after the lesion(s) are removed (He et al., 2016). Selective estrogen receptor modulators (Pluchino and Taylor, 2016), GnRH agonists (Ham et al., 2019), aromatase inhibitors or progestins are used to reduce circulating estrogen levels, but the possible harms of decreased estrogen to fertility are due to the effects of aromatase inhibitors on various diseases such as osteoporosis and osteopenia. Considering the fact that some patients do not respond to progestins due to progesterone resistance (Patel et al., 2018), there is a need to develop more effective treatments with minimized side effects by revealing the main mechanism of formation of the disease.

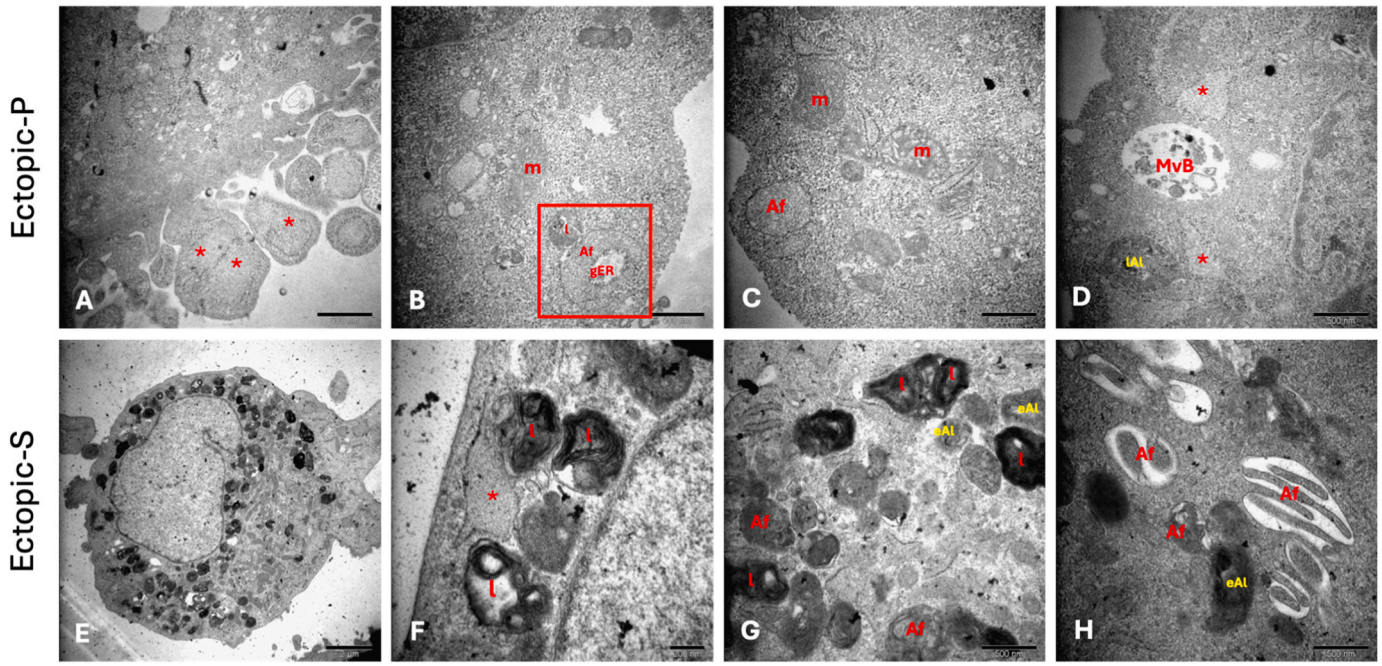


Fig. 14. Electron microscopic photomicrographs of the ectopic eMSCs in proliferative **(A-D)** and secretory phases **(E-H)**. red star: enlarged ER sacs; l: lysosome; Af: autophagosome; eAl: early autolysosome; lAl: late autolysosome; red frame: fusing of gER-containing autophagosome with lysosome (ERphagy); MvB: multivesicular body; m: mitochondrion. Uranyl acetate and lead citrate. Scale bar: A-D, G-H: 500 nm; F: 200 μm; E: 2 μm.

The most common method for diagnosing the disease is laparoscopy, but this method has disadvantages. Trauma to the patient, high cost of the procedure, potential risks after anesthesia, visceral tissue and vascular injuries are some of these disadvantages. Additionally, this method is insufficient to detect deep or invisible lesions. Therefore, there is a need for non-invasive serological tests that are more preferred by both the patient and the doctor. However, today there is no effective and sufficient serological test alone for the diagnosis of endometriosis (Liu et al., 2020).

When the theories put forward regarding the etiology of the disease are examined; the theory of retrograde menstruation, which describes the spread of endometrial tissue from the fallopian tubes into the peritoneal cavity, is the first and most accepted theory (Sampson, 1927). According to this theory, endometrial tissue pieces that pass from the tubes to the abdominal cavity adhere to the peritoneal mesothelium and then develop blood vessels to maintain their vitality and grow (Giudice and Kao, 2004). However, this theory cannot explain why endometriosis develops in 10 % of women even though 76–90 % of them menstruate, and why endometriosis occurs in men (Rei et al., 2018) and in distant organs that are not related to the peritoneum (Laganà et al., 2019). Therefore, the retrograde menstruation theory is insufficient alone to explain the pathogenesis. Hypotheses developed in line with recent studies state that endometriosis pathology is caused by stem cells (Pluchino and Taylor, 2016). Cellular damage caused by inflammatory cytokines and ROS triggers the activation of endometrial stem cells, which induce local estrogen production. Therefore, endometrial stem cells are thought to play a role in the etiopathology of benign and malignant diseases such as endometriosis, endometrial hyperplasia and endometrial cancer. These cells increase the expression of anti-apoptotic Bcl-2, the Wnt-beta catenin pathway, and the expression of cell cycle regulator genes to repair DNA damage (Maruyama and Yoshimura, 2012; Masuda et al., 2010). In addition, endometriotic lesions attract the already small number of stem cells in the circulation like a sponge, reducing the stem cell reserve of the uterus, which affects the formation of endometrial defects (Pluchino and Taylor, 2016). Considering all these findings, it is concluded that stem cells are involved in the etiopathology of endometriosis and are even one of the main factors that create the pathology, and that these stem cells, which constitute the origin of the disease, should be focused on. ER stress is a protection mechanism that cells use to rescue the cell under stress conditions. To cope with ER stress, the cell initiates the UPR, in which the expression of ER chaperones increases, the translation level of general proteins decreases, and misfolded proteins are degraded. When ER stress is prolonged, ER stress-mediated apoptosis is initiated. There are three well-known apoptotic pathways: extrinsic, intrinsic and perforin/granzyme pathway. In the intrinsic pathway, PERK activates CHOP and B-cell lymphoma-2 (Bcl-2) is negatively regulated. Additionally, ASK1 and JNK pathways are triggered by IRE1. Finally, released cytochrome C initiates apoptosome formation, resulting in activation of caspase-9 and the caspase cascade. It has been shown in many studies that ER stress-related responses play a role in the pathology of various diseases, including endometriosis. There are some, albeit limited, studies on ER stress in endometriosis, but these studies are on mature (somatic) stromal or epithelial cells. In the literature review, no study was found investigating ER stress in eMSCs in endometriosis cases. In our study, eMSCs obtained from healthy and endometriosis tissues were compared for the first time with proteomics analysis, and the proteins that are effective in ER stress in these cells were revealed. When the findings obtained from the study are evaluated; eMSCs isolated from endometrial and endometriotic tissue in healthy and patient groups; in addition to osteogenic, adipogenic and chondrogenic differentiation findings, characterization results by flow cytometry prove that successful eMSC isolation has been achieved (Gargett et al., 2016; Dominici et al., 2006; Ciuffreda et al., 2016).

As a result of proteomics analysis, when eutopic and ectopic endometrium groups of the proliferative phase were compared with the control group; ERp44, RTN3 and TMED2 increased in the eutopic group; RTN3 and TMED2 increased in the ectopic group. It was determined that ERp44 level was higher in the eutopic group than in the ectopic group. In addition to these findings; TMEM33 and TMX3 protein levels were decreased in the eutopic and ectopic endometrium group compared to the control group. When the eutopic and ectopic groups were compared, TMEM33, TMED2 and RTN3 levels were decreased in the eutopic group compared to the ectopic group.

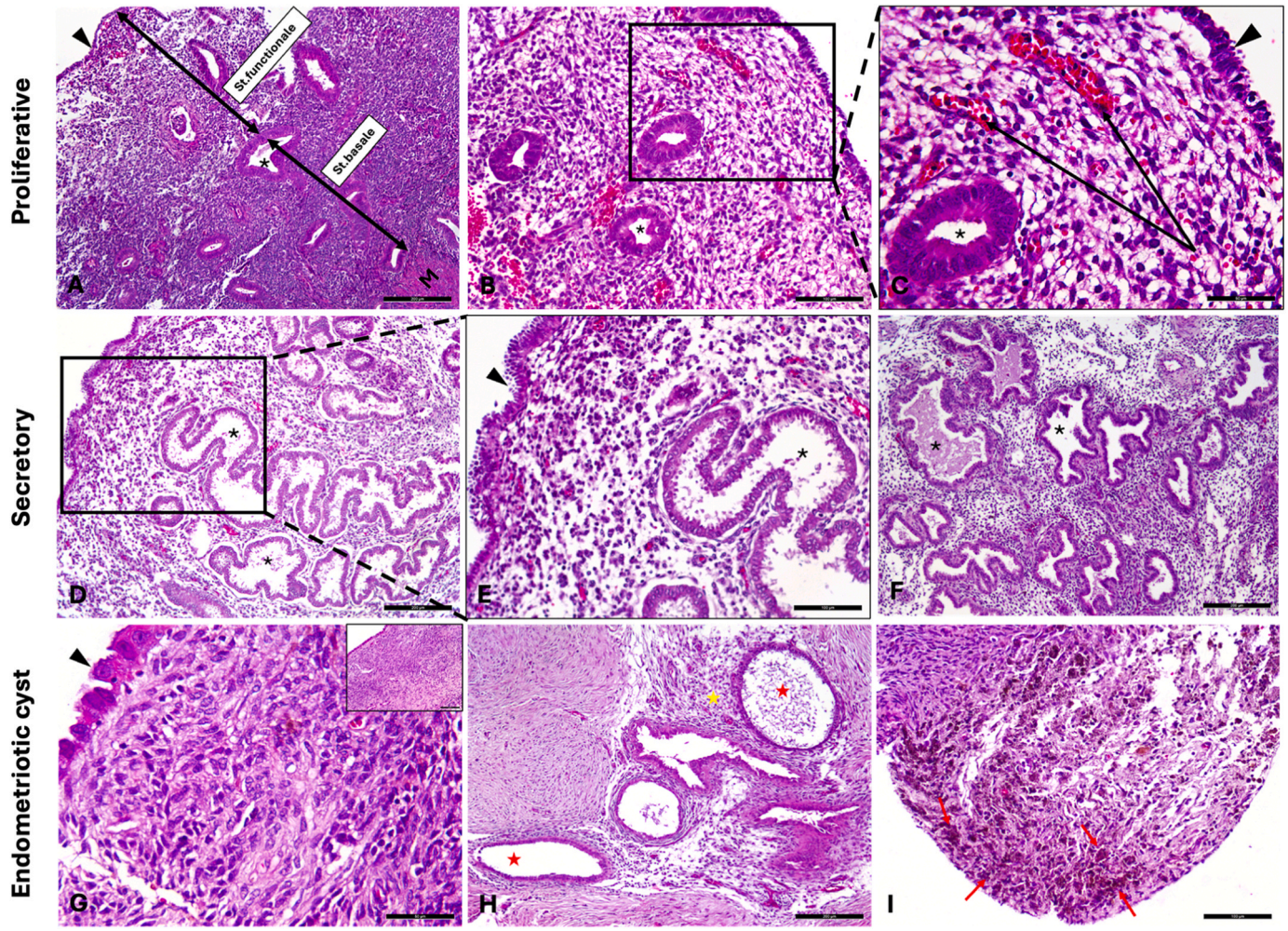


Fig. 15. H&E photomicrographs of endometrial and endometriotic tissue sections belonging to proliferative and secretory phases. Black arrow: blood vessel; black star: endometrial gland; arrow head: endometrial epithelium; red star: endometrium like gland; red arrow: hemosiderin granules; M: Myometrium. H&E. Scale bar: A, D, F, H: 200 μm; E, I: 100 μm; C, G: 50 μm.

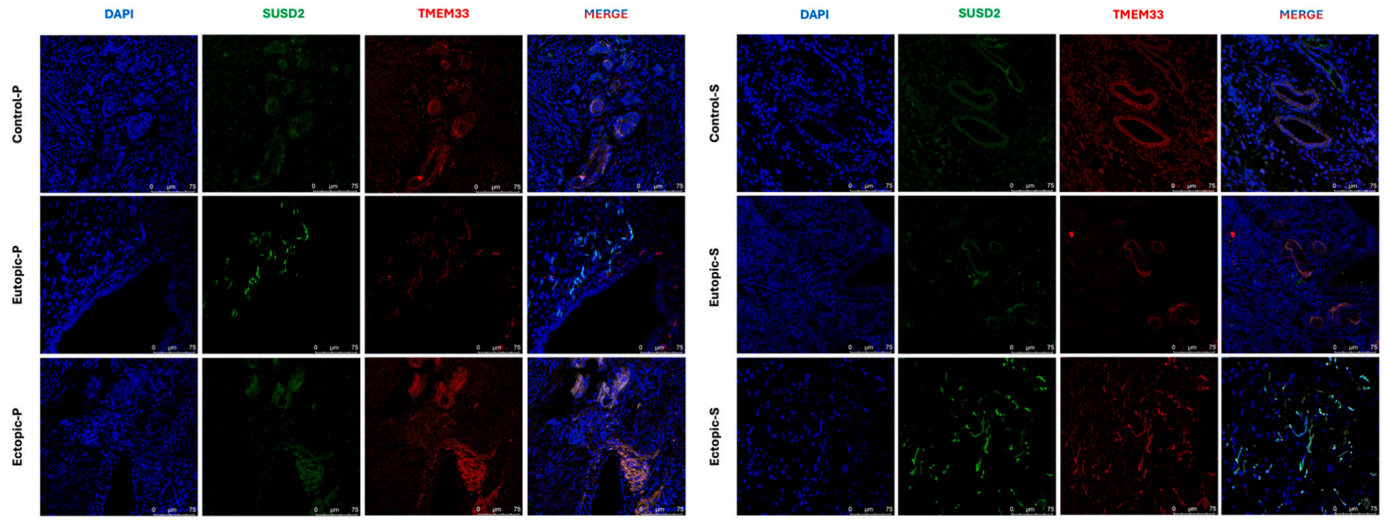


Fig. 16. TMEM33 expression in control, eutopic and ectopic endometrium groups belonging to the proliferative and secretory phases. Scale bar: 75 μm.

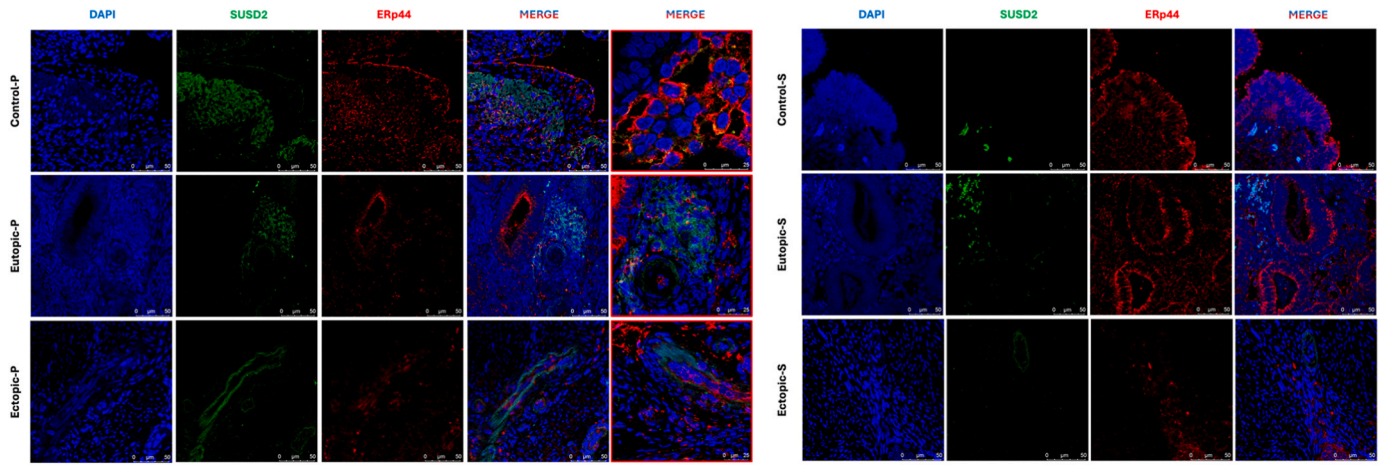


Fig. 17. ERp44 expression in control, eutopic and ectopic endometrium groups belonging to the proliferative and secretory phases. Scale bar: 50 μm. Photomicrographs framed in red contain higher magnification images of the relevant group (Scale bar: 25 μm).

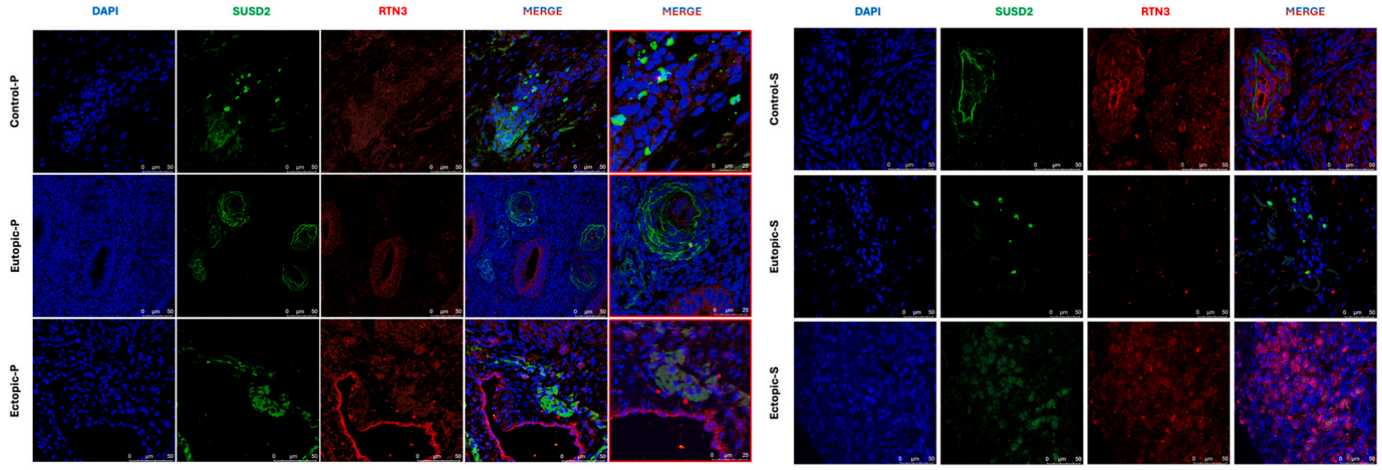


Fig. 18. RTN3 expression in control, eutopic and ectopic endometrium groups belonging to the proliferative and secretory phases. Scale bar: 50 μm. Photomicrographs framed in red contain higher magnification images of the relevant group (Scale bar: 25 μm).

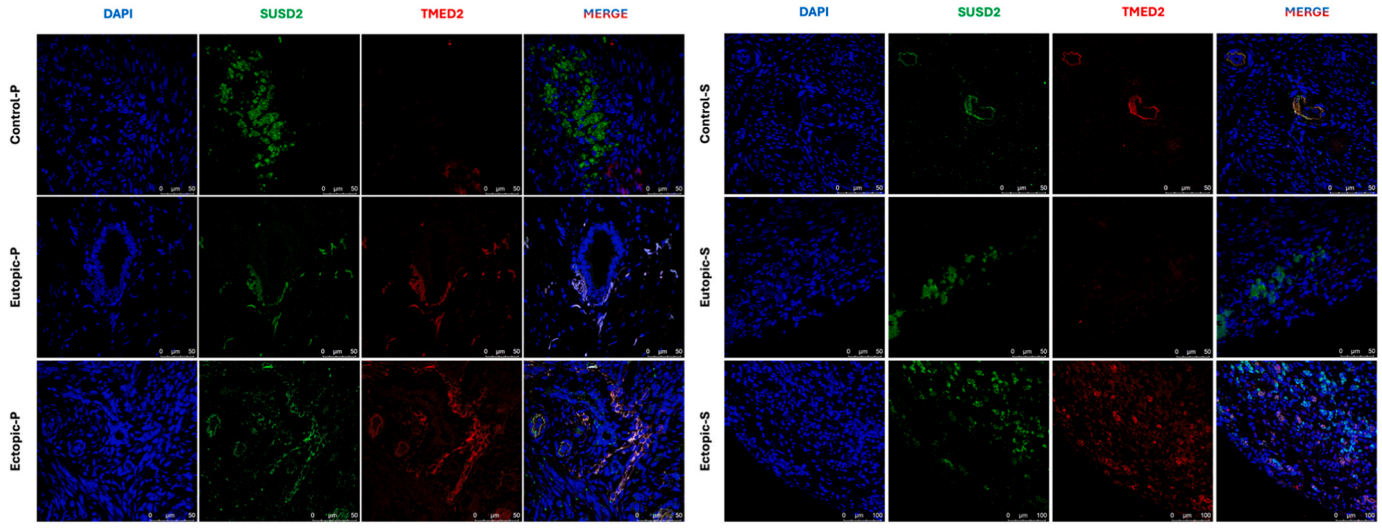


Fig. 19. TMED2 expression in control, eutopic and ectopic endometrium groups belonging to the proliferative and secretory phases. Scale bar: 50 μm.

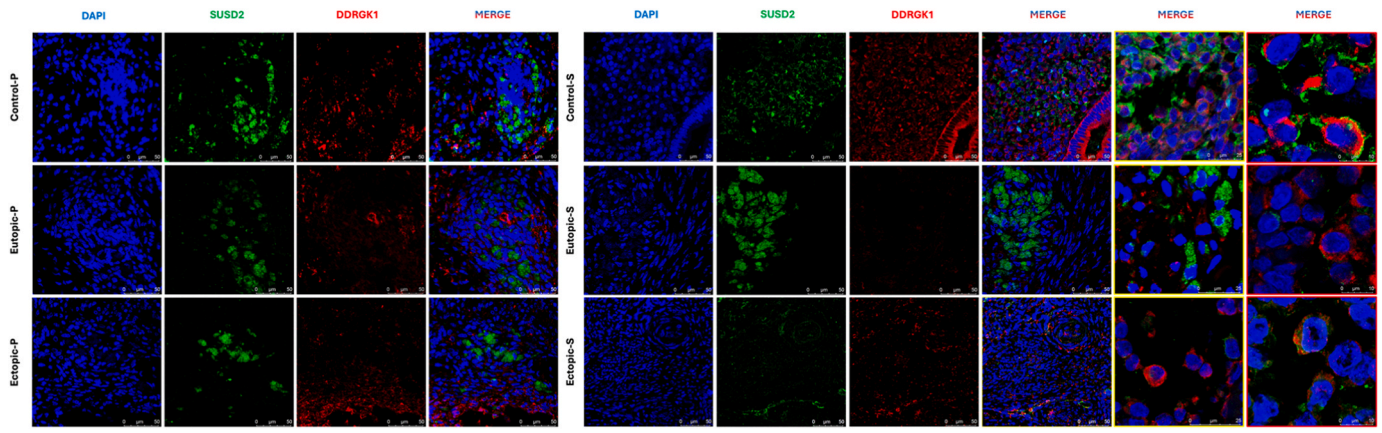


Fig. 20. DDRGK1 expression in control, eutopic and ectopic endometrium groups belonging to the proliferative and secretory phases. Scale bar: 50 μm. Photomicrographs framed in red contain higher magnification images of the relevant group (Scale bar: 25 μm).

ERp44 is a molecule that exhibits multifunctional chaperone activity related to the PDI family. The formation of disulfide bonds is essential for the folding and biological activity of most secretory and membrane proteins (Anelli et al., 2002). In addition, ERp44 is involved in intracellular Ca^{+2} release (Higo et al., 2005), maturation of secretory proteins in the ER, cardiac development (Wang et al., 2014), control of blood pressure (Hisatsune et al., 2015) and ER stress. It has been shown to participate in other activities such as protein activation. However, in the literature, related to ER stress in endometriosis; no study has investigated ERp44 expression in epithelial, stromal or stem cells. Pang et al. reported that the absence of ERp44 exacerbates ER stress in diabetic nephropathy (Pang et al., 2018). Chang et al. reported that when ERp44 is silenced, ER stress is activated and causes cell apoptosis (Chang et al., 2015). When the proteome data obtained from our study was evaluated, ERp44 was expressed most in the eutopic endometrium in the proliferative phase. Considering the important role of ERp44 in protein folding; it is an expected result that translation increases in the endometriosis group, where ER stress increases and folding proteins are required more. In the ectopic endometrium group, another group in which ER stress is observed, ERp44 decreased significantly compared to the eutopic group and there was no significant difference with the control group. This data suggest that ERp44 is not involved in the stress pathway in ectopic endometrium. These findings also coincide with immunofluorescence and western blot analysis results. When the gene expression analysis of ERp44 was evaluated, it decreased in the eutopic and ectopic endometrium groups compared to the control group. The reason for this decrease in the gene level may be due to the negative feedback mechanism in ERp44 in the eutopic endometrium, which reduces its own mRNA transcription by ERp44, whose translation increases. When the proteomics analysis of RTN3 is examined; RTN3 expression increased in endometriosis groups (especially in the ectopic group) compared to the control group. Western blot and immunofluorescence analysis results and gene expression analysis also confirm the increase in RTN3 protein in the ectopic endometrium group. It has been reported that RTN3 functions as a selective receptor in the autophagic pathway and is involved in the lysosomal degradation of ER fragments by interacting with LC3 (Grumati et al., 2017). In addition, it has been reported that RTN3 is activated under ER stress and increases Beclin-1-dependent autophagy by interacting with Bcl-2 (Chen et al., 2011). The autophagolysosome structures seen in the ectopic endometrium group in our study (Fig. 13) are compatible with the literature findings above and reveal the relationship between ER stress and autophagy.

ER involves two interconnected quality control pathways: UPR and ER-associated degradation (ERAD). UPR activation increases the folding capacity of the ER, while the ERAD system recognizes misfolded proteins and facilitates their retro-translocation to the cytoplasm, where they are degraded by the ubiquitin-proteasome system. ER also plays an active role in the cell's secondary main degradative system: the autophagy-lysosome pathway. Autophagy is a catabolic process characterized by the formation of a double-membrane structure called an autophagosome, which engulfs cytosolic fractions (such as protein aggregates and organelles) and delivers them to the lysosome. ER, the largest membrane-bound organelle, serves as the main membrane source for autophagosome formation (Grumati et al., 2017). In the ERAD pathway, misfolded proteins pass to the cytoplasm via Sec61, where they are ubiquitinated and degraded by 26S proteasomes. Receptors such as FAM134B, SEC62 and RTN3 are involved in ERphagy/reticulophagy, which is a type of autophagy (Bhardwaj et al., 2020). In our study, the expression of ERphagy-related RTN3 increased in the ectopic group at proliferative phase (Fig. 3), whereas ERAD-related Sec61 and 26S proteasome expression is decreased (Supplemantary Fig. 1). This data suggests that the ERphagy pathway is used instead of ERAD in ER stress in endometriosis. ERphagy, autophagolysosome (Fig. 13 and Fig. 14) and multivesicular body (Fig. 14) structures (Fader and Colombo, 2009) seen in eutopic and ectopic endometrium groups of the proliferative phase also support these findings at the ultrastructural level.

TMED2 is a molecule that regulates the transport of cargo proteins. Abnormal expression of this molecule causes uncontrolled protein transport (Spano and Colanzi, 2022). It has been reported that TMED2 increases the migration and invasion of ovarian cancer cells (Shi-Peng et al., 2017). In the proteome findings obtained from our study, TMED2 expression was significantly increased in the eutopic and ectopic endometrium groups in the proliferative phase compared to the control group. In immunofluorescence, western blot and RT-qPCR analysis, this increase was found to be statistically significant in the ectopic group. Similar to the behavior of ovarian cancer cells, TMED2 may play a role in the higher invasion and migration capacity of ectopic eMSCs compared to eutopic eMSCs in endometriosis (Gargett et al., 2016). In addition, the fact that abnormal expression of TMED2 causes uncontrolled protein transport suggests that it may lead to ER stress. This coincides with increased TMED2 expression in endometriosis groups, especially ectopic group. In the limited number of studies in the literature investigating TMED2 and ER stress, it has been reported that deletion or mutation of TMED genes in yeast and Drosophila results in ER stress and UPR activation (Hou et al., 2017). Since TMED2 is a cargo protein, it is an expected result that its expression increased under ER stress in our study. However, in the study conducted by Hou et al., ER stress develops due to the absence/defect of TMED2, one of the molecules involved in protein transport, as a result of deletion or mutation. Therefore, it can be hypothesized that overexpression or lack of expression of TMED2 is associated with ER stress.

TMEM33 (also known as DB83) is a transmembrane protein, and recent studies have reported that this protein, which is induced by ER stress in the cell, is responsible for the regulation of PERK and IRE1α (Sakabe et al., 2015). When the proliferative phase TMEM33 proteomics data of our study is evaluated; a significant decrease was detected in the eutopic group compared to the control and ectopic groups. While the immunofluorescence analysis results supported the proteome data, in the gene expression analysis, only the increase of TMEM33 in the ectopic endometrium group was found to be significant compared to the eutopic group. It has been found that overexpression of TMEM33 in breast cancer cells increases the expression of both peIF2α and pIRE1α. Again, overexpression of TMEM33 in these cells caused increased expression of CHOP, ATF4, XBP1-S, active caspase-7 and LC3II, an autophagosome marker (Sakabe et al., 2015). In our study; The PERK and IRE1α gene expression levels, which increased simultaneously with the TMEM33 protein level in the ectopic endometrium group of the proliferative phase, is consistent with the literature information above. Similarly, in the ultrastructural analysis of our study, the increased number of autophagosomes in endometriosis groups is consistent with the increase in LC3II in the literature. The appearance of enlarged gER vesicles, one of the morphological markers of ER stress, parallels the presence of ER stress in these cells (Akiyama et al., 2009; Liu et al., 2019) and the increase in TMEM33 induced by this stress (Sakabe et al., 2015). Although the role of TMX3, which belongs to the PDI family, in cells is not known exactly, it has been reported that it reduces the stress state by protecting cells against neuronal atrophy in the Huntington's disease model, where ER stress is triggered (Fox et al., 2015). In our study, when TMX3 expression was analyzed at the gene level in the proliferative phase; a significant decrease was detected in the eutopic group compared to the control group. This finding is consistent with proteome data. However, while an increase was observed in the ectopic group in gene analysis, a decrease was observed in proteomic analysis. The decreased TMX3 protein and mRNA levels observed in eutopic endometrium compared to the control led to the thought that TMX3 may not be effective in coping with ER stress in this group. However, when looking at the ectopic endometrium group, gene expression is high but protein expression is low. It points to mechanisms that are disrupted at the post-transcriptional or post-translational stage.

When the data regarding the DDRGK1 molecule is examined; significant differences were detected in western blot, immunofluorescence and RT-qPCR analysis in eutopic and ectopic endometrium groups in both proliferative and secretory phases compared to their controls. In the proteome data, this significance was only seen in the secretory phase. When the groups belonging to the proliferative phase are examined; western blot and immunofluorescence analysis results of DDRGK1, which showed a significant decrease in the eutopic and ectopic endometrium groups compared to the control group, are parallel to each other. RT-qPCR analysis indicates the opposite of these results. Increased DDRGK1 gene expression was detected in eutopic and ectopic endometrium groups in the proliferative phase compared to the control group. This may be due to the effectiveness of the negative feedback mechanism.

When the control, eutopic and ectopic endometrium groups of the secretory phase were examined, it was determined that DDRGK1 showed a significant decrease in the eutopic and ectopic groups compared to the control group. Likewise, while western blot and immunofluorescence analyzes support this finding at the protein level, this finding is not supported at the gene expression level. Increased DDRGK1 gene expression was detected in the ectopic endometrium group of the secretory stage compared to the control. This data, which is similar to the proliferative phase results, leads to the inference that there is a negative feedback relationship between the protein and gene level of DDRGK1. Studies have reported that DDRGK1 depletion suppresses UPR-IRE1a signaling and activates the UPR-PERK apoptotic pathway. Supporting this result, p-eIF2α and CHOP expression also increased (Liu et al., 2017). Additionally, DDRGK1 regulates IRE1a protein stabilization in the breast cancer cell line through ubiquitylation-dependent protein-protein interaction and has an important role in the maintenance of ER homeostasis. It was also determined that when the DDRGK1 gene was silenced in these cells, the total IRE1α level decreased, but phosphorylated IRE1 α (p-IRE1α) decreased slightly. The level of ATF6 or cleaved ATF6 was unchanged; total PERK level did not change, but p-PERK and GRP78 levels increased (Stephani et al., 2020). Similar to the literature findings, an increase in GRP78, PERK and IRE1α gene expression was observed in the ectopic endometrium group of the proliferative phase, while no significant difference was observed in the ATF6 level. Although there was an increase in ectopic GRP78 expression compared to the control in immunofluorescence and western blot analyses, this increase was not found to be statistically significant. When the secretory phase was examined, it was determined that only IRE1α and PERK increased in the ectopic endometrium group compared to the control.

DDRGK1 is a molecule involved in ubiquitylation in reticulophagy. Uphimylation-dependent reticulophagy inhibits the UPR pathway by regulating ERN1/ IRE1α stabilization. The decrease in the level of this molecule in endometriosis groups shows that it cannot inhibit the UPR pathway. Increased IRE1α gene expression in the ectopic group in RT-qPCR analysis also supports this finding.

To cope with ER stress, the cell initiates the UPR, in which the expression of ER chaperones increases, the translation level of general proteins decreases, and misfolded proteins are degraded. When ER stress is prolonged, ER stress-mediated apoptosis is initiated. There are three well-known apoptotic pathways: extrinsic, intrinsic and perforin/granzyme pathways. In the intrinsic pathway, PERK activates CHOP and B-cell lymphoma-2 (Bcl-2) is negatively regulated. Additionally, ASK1 and JNK pathways are triggered by IRE1. Finally, released cytochrome C initiates apoptosome formation, resulting in activation of caspase-9 and the caspase cascade. In our study, when the proteome, immunofluorescence and western blot data were examined, no significant difference was seen at the protein level in GRP78 and the three main molecules involved in the UPR. However, when looked at at the gene level, increased expression of PERK and IRE1α was observed in both proliferative and secretory phases, especially in the ectopic endometrium. However, no significant difference was observed in terms of ATF6 in both stages. This suggests that the ER stress seen in endometriosis is mostly effective through the PERK and IRE1α pathways. The fact that the statistically significant increase of these molecules at the gene level is not reflected at the protein level (in terms of GRP78) may be due to the short half-life of the proteins, the stress of the cells in the culture environment may decrease, or the disorders occurring at the post-transcriptional or post-translational level. Although there is no study in the literature about ER stress of eMSCs in endometriosis, there are several studies on stromal cells. These studies focused mostly on the main UPR pathway. When the relationship of UPR molecules and apoptosis-related molecules with endometriosis is examined, Bcl-2 and Bcl-xL expression is higher in ectopic endometrium than in eutopic and healthy endometrium (Delbandi et al., 2020), GRP78 and CHOP expression is lower in the late secretory phase than in healthy endometrium (Choi et al., 2019). It has been reported that GRP78 and xBP1 expression is higher in eutopic endometrium than in ectopic endometrium, CHOP expression does not change, and ATF6 is expressed more in eutopic and ectopic endometrium than in healthy endometrium (Ciavattini et al., 2018). It has also been reported that IKK suppresses apoptosis in endometriotic cells by phosphorylating Bad, which is a Bcl-2 antagonist (Kocbek et al., 2016). In the study conducted by Liang et al., it was reported that the suppression of proliferation and increase of apoptosis in endometriotic stromal cells depend on JNK activation (Liang et al., 2017). In our study, ER stress-related proteins determined as a result of proteomics analysis were studied. Although there are studies in the literature evaluating proteome analysis in endometriosis, these studies are based on protein isolation from samples such as serum, peritoneal fluid and endometrial tissue, and no distinction is made

between epithelial, stromal or stem cells (Zhang et al., 2006; Siva et al., 2014). Proteins found to be significant in relevant studies also differ from the data we obtained in our study.

When we evaluate the proteome data other than the proteins we examined; it was determined that in the eutopic endometrium during the proliferative phase, the ERO-1-like alpha protein, which prevents ROS accumulation in the ER, was significantly reduced compared to the control group. SOD, a marker of antioxidant activity, decreased in the ectopic endometrium group compared to the control group. This coincides with the increased OS levels seen in endometriosis. It also suggests that the decreased expression of PRA-1 family protein 3, a positive regulator of apoptosis, seen in these groups may be related to impaired apoptotic pathways caused by estrogen dominance and developing progesterone resistance in endometriosis. Compared to the control group, HSJ2 molecule, which protects cells from apoptosis, was found in the ectopic endometrium group. The significant decrease in PDCD6IP, one of the programmed cell death proteins, in the eutopic endometrium group may be related to the impaired apoptotic pathways seen in endometriosis (Supplementary Figure 2).

As a result, it was determined that there was a significant difference in ER stress-related proteins in eMSCs in eutopic and ectopic endometriosis groups, especially in the proliferative phase, compared to the control group, and the relationship of these cells with autophagic pathways related to ER stress was revealed. These findings, evaluated at the protein and gene level, were also supported by the dilated/widened gER vesicles and reticulophagy structures seen in ultrastructural examination.

Considering the financial limitations of our study, western blot, immunofluorescence and RT-qPCR analysis of more proteins should be performed to confirm the extensive proteome data. Expanding the sample pool by increasing the number of patients in the groups and including molecular analyzes such as gene silencing experiments in future studies will make a greater contribution to elucidating this pathology.

Disclosures

The authors of this study confirmed that they had no conflicts of interest that could have influenced the results. This study was approved by the Kocaeli University Ethical Committee of Non-Invasive Clinical Research (Project no: 2020/551) and all participants signed written informed consent before participating in the study.

Disclosures and author statement

The authors of this study confirmed that they had no conflicts of interest that could have influenced the results.

CRediT authorship contribution statement

Gokhan Duruksu: Validation, Methodology, Investigation, Formal analysis. Gurler **Akpınar:** Methodology, Investigation, Formal analysis. **Elif Guzel:** Methodology, Investigation, Formal analysis. **Zehra Sezer:** Methodology, Investigation. **Mehmet Sarıhan:** Methodology, Investigation. **Ahmet Ozturk:** Methodology, Investigation. **Zeynep Ece Utkan Korun:** Methodology, Investigation. **Aydın Corakci:** Methodology, Investigation. **Yusufhan Yazir:** Writing – review & editing, Writing – original draft, Supervision, Project administration, Methodology, Investigation, Funding acquisition, Formal analysis, Conceptualization. **Selenay Furat Rencber:** Writing – review & editing, Writing – original draft, Visualization, Validation, Resources, Methodology, Investigation, Formal analysis, Data curation, Conceptualization.

Data Availability

Data will be made available on request.

Acknowledgement

All procedures in this study confirmed to the Declaration of Helsinki and Institutional Review Board (Medical Ethical Committee, Kocaeli University Medical Faculty, Kocaeli, Turkey). We thanks to Kocaeli University Scientific Research Projects Coordination Unit in terms of financially supporting for this study through a project (KOU-BAP: Project No: TDK-2020-2223). In addition, Scientific and Technological Research Council of Turkey (TUBITAK) financially supported this study through a project (Project No:321S003).

Appendix A. Supporting information

Supplementary data associated with this article can be found in the online version at doi:10.1016/j.tice.2024.102544.

References

Akiyama, M., Hatanaka, M., Ohta, Y., Ueda, K., Yanai, A., Uehara, Y., Tanabe, K., Tsuru, M., Miyazaki, M., Saeki, S., Saito, T., Shinoda, K., Oka, Y., Tanizawa, Y., 2009. Increased insulin demand promotes while pioglitazone prevents pancreatic beta cell apoptosis in Wfs1 knockout mice. Diabetologia *52* (4), 653–663. https://doi.org/10.1007/s00125-009-1270-6.

Anelli, T., Alessio, M., Mezghrani, A., Simmen, T., Talamo, F., Bachi, A., Sitia, R., 2002. ERp44, a novel endoplasmic reticulum folding assistant of the thioredoxin family. EMBO J. *21* (4), 835–844. https://doi.org/10.1093/emboj/21.4.835.

Barragan, F., Irwin, J.C., Balayan, S., Erikson, D.W., Chen, J.C., Houshdaran, S., Piltonen, T.T., Spitzer, T.L., George, A., Rabban, J.T., Nezhat, C., Giudice, L.C., 2016. Human Endometrial Fibroblasts Derived from Mesenchymal Progenitors Inherit Progesterone Resistance and Acquire an Inflammatory Phenotype in the Endometrial Niche in Endometriosis. Biol. Reprod. *94* (5), 118. https://doi.org/10.1095/biolreprod.115.136010.

Bhardwaj, M., Leli, N.M., Koumenis, C., Amaravadi, R.K., 2020. Regulation of autophagy by canonical and non-canonical ER stress responses. Semin. Cancer Biol. *66*, 116–128. https://doi.org/10.1016/j.semcancer.2019.11.007.

Cao, H., Wei, Y.X., Zhou, Q., Zhang, Y., Guo, X.P., Zhang, J., 2017. Inhibitory effect of curcumin in human endometriosis endometrial cells via downregulation of vascular endothelial growth factor. Mol. Med. Rep. *16* (4), 5611–5617. https://doi.org/10.3892/mmr.2017.7250.

Chang, Y., Wu, Y., Liu, W., Ji, G., 2015. Knockdown of ERp44 leads to apoptosis via activation of ER stress in HeLa cells. Biochem. Biophys. Res. Commun. *463* (4), 606–611. https://doi.org/10.1016/j.bbrc.2015.05.106.

Chen, R., Jin, R., Wu, L., Ye, X., Yang, Y., Luo, K., Wang, W., Wu, D., Ye, X., Huang, L., Huang, T., Xiao, G., 2011. Reticulon 3 attenuates the clearance of cytosolic prion aggregates via inhibiting autophagy. Autophagy *7* (2), 205–216. https://doi.org/10.4161/auto.7.2.14197.

Choi, J.Y., Jo, M.W., Lee, E.Y., Lee, D.Y., Choi, D.S., 2018. Ovarian steroid dependence of endoplasmic reticulum stress involvement in endometrial cell apoptosis during the human endometrial cycle. Reprod. (Camb., Engl.) *155* (6), 493–503. https://doi.org/10.1530/REP-17-0713.

Choi, J., Jo, M., Lee, E., Lee, D.Y., Choi, D., 2019. Involvement of endoplasmic reticulum stress in regulation of endometrial stromal cell invasiveness: possible role in pathogenesis of endometriosis. Mol. Hum. Reprod. *25* (3), 101–110. https://doi.org/10.1093/molehr/gaz002.

Ciavattini, A., Delli Carpini, G., Serri, M., Tozzi, A., Leoni, F., Di Loreto, E., Saccucci, F., 2018. Unfolded protein response, a link between endometrioid ovarian carcinoma and endometriosis: A pilot study. Oncol. Lett. *16* (4), 5449–5454. https://doi.org/10.3892/ol.2018.9256.

Ciuffreda, M.C., Malpasso, G., Musarò, P., Turco, V., Gnecchi, M., 2016. Protocols for in vitro Differentiation of Human Mesenchymal Stem Cells into Osteogenic, Chondrogenic and Adipogenic Lineages. Methods Mol. Biol. (Clifton, N. J.) *1416*, 149–158. https://doi.org/10.1007/978-1-4939-3584-0_8.

Clement, P.B., 2007. The pathology of endometriosis: a survey of the many faces of a common disease emphasizing diagnostic pitfalls and unusual and newly appreciated aspects. Adv. Anat. Pathol. *14* (4), 241–260. https://doi.org/10.1097/PAP.0b013e3180ca7d7b.

Cousins, F.L., O, D.F., Gargett, C.E., 2018. Endometrial stem/progenitor cells and their role in the pathogenesis of endometriosis. Best. Pract. Res. Clin. Obstet. Gynaecol. *50*, 27–38. https://doi.org/10.1016/j.bpobgyn.2018.01.011.

Delbandi, A.A., Mahmoudi, M., Shervin, A., Heidari, S., Kolahdouz-Mohammadi, R., Zarnani, A.H., 2020. Evaluation of apoptosis and angiogenesis in ectopic and eutopic stromal cells of patients with endometriosis compared to non-endometriotic controls. BMC Women'S. Health *20* (1), 3. https://doi.org/10.1186/s12905-019-0865-4.

Dominici, M., Le Blanc, K., Mueller, I., Slaper-Cortenbach, I., Marini, F., Krause, D., Deans, R., Keating, A., Prockop, Dj, Horwitz, E., 2006. Minimal criteria for defining multipotent mesenchymal stromal cells. The International Society for Cellular Therapy position statement. Cytotherapy *8* (4), 315–317. https://doi.org/10.1080/14653240600855905.

Ekiz-Yilmaz, T., Isildar, B., Gezer, A., Kankaya, D., Cansiz-Ersoz, C., Kayisli, U.A., Guzel, E., 2021. The role of unfolded protein response in the pathogenesis of

endometriosis: contribution of peritoneal fluid. Reprod. Biomed. Online 42 (1), 1–15. https://doi.org/10.1016/j.rbmo.2020.09.012.
Fader, C.M., Colombo, M.I., 2009. Autophagy and multivesicular bodies: two closely related partners. Cell death Differ. *16* (1), 70–78. https://doi.org/10.1038/cdd.2008.168.
Fox, J., Lu, Z., Barrows, L., 2015. Thiol-disulfide Oxidoreductases TRX1 and TMX3 Decrease Neuronal Atrophy in a Lentiviral Mouse Model of Huntington's Disease. ecurrents.hd.b966ec2eca8e2d89d2bb4d020be4351e PLoS Curr. 7. https://doi.org/10.1371/currents.hd.b966ec2eca8e2d89d2bb4d020be4351e.
Gargett, C.E., Schwab, K.E., Deane, J.A., 2016. Endometrial stem/progenitor cells: the first 10 years. Hum. Reprod. Update *22* (2), 137–163. https://doi.org/10.1093/humupd/dmv051.
Giudice, L.C., Kao, L.C., 2004. Endometriosis. Lancet (Lond., Engl.) *364* (9447), 1789–1799. https://doi.org/10.1016/S0140-6736(04)17403-5.
Grumati, P., Morozzi, G., Hölper, S., Mari, M., Harwardt, M.I., Yan, R., Müller, S., Reggiori, F., Heilemann, M., Dikic, I., 2017. Full length RTN3 regulates turnover of tubular endoplasmic reticulum via selective autophagy. eLife *6*, e25555. https://doi.org/10.7554/eLife.25555.
Guzel, E., Arlier, S., Guzeloglu-Kayisli, O., Tabak, M.S., Ekiz, T., Semerci, N., Larsen, K., Schatz, F., Lockwood, C.J., Kayisli, U.A., 2017. Endoplasmic Reticulum Stress and Homeostasis in Reproductive Physiology and Pathology. Int. J. Mol. Sci. *18* (4), 792. https://doi.org/10.3390/ijms18040792.
Ham, J., Kim, J., Bazer, F.W., Lim, W., Song, G., 2019. Silibinin-induced endoplasmic reticulum stress and mitochondrial dysfunction suppress growth of endometriotic lesions. J. Cell. Physiol. *234* (4), 4327–4341. https://doi.org/10.1002/jcp.27212.
He, H., Liu, R., Xiong, W., Pu, D., Wang, S., Li, T., 2016. Lentiviral vector-mediated down-regulation of Notch1 in endometrial stem cells results in proliferation and migration in endometriosis. Mol. Cell. Endocrinol. *434*, 210–218. https://doi.org/10.1016/j.mce.2016.07.004.
Higo, T., Hattori, M., Nakamura, T., Natsume, T., Michikawa, T., Mikoshiba, K., 2005. Subtype-specific and ER lumenal environment-dependent regulation of inositol 1,4,5-trisphosphate receptor type 1 by ERp44. Cell *120* (1), 85–98. https://doi.org/10.1016/j.cell.2004.11.048.
Hisatsune, C., Ebisui, E., Usui, M., Ogawa, N., Suzuki, A., Mataga, N., Takahashi-Iwanaga, H., Mikoshiba, K., 2015. ERp44 Exerts Redox-Dependent Control of Blood Pressure at the ER. Mol. Cell *58* (6), 1015–1027. https://doi.org/10.1016/j.molcel.2015.04.008.
Hou, W., Gupta, S., Beauchamp, M.C., Yuan, L., Jerome-Majewska, L.A., 2017. Non-alcoholic fatty liver disease in mice with heterozygous mutation in TMED2. PloS One *12* (8), e0182995. https://doi.org/10.1371/journal.pone.0182995.
Hufnagel, D., Li, F., Cosar, E., Krikun, G., Taylor, H.S., 2015. The Role of Stem Cells in the Etiology and Pathophysiology of Endometriosis. Semin. Reprod. Med. *33* (5), 333–340. https://doi.org/10.1055/s-0035-1564609.
Karaoz, E., Aksoy, A., Ayhan, S., Sariboyaci, A.E., Kaymaz, F., Kasap, M., 2009. Characterization of mesenchymal stem cells from rat bone marrow: ultrastructural properties, differentiation potential and immunophenotypic markers. Histochem. Cell Biol. *132* (5), 533–546. https://doi.org/10.1007/s00418-009-0629-6.
Kiliç, K.C., Yazir, Y., Öztürk, A., Halbutoğullari, Z.S., Mert, S., Gacar, G., Duruksu, G., 2023. Investigation of impacts of decellularized heart extracellular matrix and VEGF on cardiomyogenic differentiation of mesenchymal stem cell through Notch/Hedgehog signaling pathways. Tissue Cell 84, 102195. https://doi.org/10.1016/j.tice.2023.102195.
Kocbek, V., Grandi, G., Blank, F., Wotzkow, C., Bersinger, N.A., Mueller, M.D., Kyo, S., McKinnon, B.D., 2016. TNFα-induced IKKβ complex activation influences epithelial, but not stromal cell survival in endometriosis. Mol. Hum. Reprod. *22* (11), 768–777. https://doi.org/10.1093/molehr/gaw054.
Laganà, A.S., Garzon, S., Götte, M., Viganò, P., Franchi, M., Ghezzi, F., Martin, D.C., 2019. The Pathogenesis of Endometriosis: Molecular and Cell Biology Insights. Int. J. Mol. Sci. *20* (22), 5615. https://doi.org/10.3390/ijms20225615.
Lessey, B.A., Kim, J.J., 2017. Endometrial receptivity in the eutopic endometrium of women with endometriosis: it is affected, and let me show you why. Fertil. Steril. *108* (1), 19–27. https://doi.org/10.1016/j.fertnstert.2017.05.031.
Liang, R.N., Li, P.S., Zou, Y., Liu, Y.L., Jiang, Z., Liu, Z., Fan, P., Xu, L., Peng, J.H., Sun, X. Y., 2017. Ping-Chong-Jiang-Ni Formula Induces Apoptosis and Inhibits Proliferation of Human Ectopic Endometrial Stromal Cells in Endometriosis via the Activation of JNK Signaling Pathway. Evid. -Based Complement. Altern. Med.: eCAM *2017*, 6489427. https://doi.org/10.1155/2017/6489427.
Liu, B., Ou, G., Chen, Y., Zhang, J., 2019. Inhibition of protein tyrosine phosphatase 1B protects against sevoflurane-induced neurotoxicity mediated by ER stress in developing brain. Brain Res. Bull. *146*, 28–39. https://doi.org/10.1016/j.brainresbull.2018.12.006.
Liu, J., Wang, Y., Song, L., Zeng, L., Yi, W., Liu, T., Chen, H., Wang, M., Ju, Z., Cong, Y.S., 2017. A critical role of DDRGK1 in endoplasmic reticulum homoeostasis via regulation of IRE1α stability. Nat. Commun. *8*, 14186 https://doi.org/10.1038/ncomms14186.
Liu, Y., Zhang, Z., Yang, F., Wang, H., Liang, S., Wang, H., Yang, J., Lin, J., 2020. The role of endometrial stem cells in the pathogenesis of endometriosis and their application to its early diagnosis. Biol. Reprod. *102* (6), 1153–1159. https://doi.org/10.1093/biolre/ioaa011.
Macer, M.L., Taylor, H.S., 2012. Endometriosis and infertility: a review of the pathogenesis and treatment of endometriosis-associated infertility. Obstet. Gynecol. Clin. North Am. *39* (4), 535–549. https://doi.org/10.1016/j.ogc.2012.10.002.
Maruyama, T., Yoshimura, Y., 2012. Stem cell theory for the pathogenesis of endometriosis. Front. Biosci. (Elite Ed.) *4* (8), 2754–2763. https://doi.org/10.2741/e589.
Masuda, H., Anwar, S.S., Bühring, H.J., Rao, J.R., Gargett, C.E., 2012. A novel marker of human endometrial mesenchymal stem-like cells. Cell Transplant. 21 (10), 2201–2214. https://doi.org/10.3727/096368911X637362.
Masuda, H., Matsuzaki, Y., Hiratsu, E., Ono, M., Nagashima, T., Kajitani, T., Arase, T., Oda, H., Uchida, H., Asada, H., Ito, M., Yoshimura, Y., Maruyama, T., Okano, H., 2010. Stem cell-like properties of the endometrial side population: implication in endometrial regeneration. PloS One *5* (4), e10387. https://doi.org/10.1371/journal.pone.0010387.
Oakes, S.A., Papa, F.R., 2015. The role of endoplasmic reticulum stress in human pathology. Annu. Rev. Pathol. *10*, 173–194. https://doi.org/10.1146/annurev-pathol-012513-104649.
Okcu, A., Yazir, Y., Şimşek, T., Mert, S., Duruksu, G., Öztürk, A., Kiliç, K.C., Akpinar, G., Kasap, M., 2023. Investigation of the effect of pancreatic decellularized matrix on encapsulated Islets of Langerhans with mesenchymal stem cells. Tissue Cell 82, 102110. https://doi.org/10.1016/j.tice.2023.102110.
Pang, X., Zhang, Y., Shi, X., Li, D., Han, J., 2018. ERp44 depletion exacerbates ER stress and aggravates diabetic nephropathy in db/db mice. Biochem. Biophys. Res. Commun. *504* (4), 921–926. https://doi.org/10.1016/j.bbrc.2018.09.037.
Patel, B.G., Lenk, E.E., Lebovic, D.I., Shu, Y., Yu, J., Taylor, R.N., 2018. Pathogenesis of endometriosis: Interaction between Endocrine and inflammatory pathways. Best. Pract. Res. Clin. Obstet. Gynaecol. *50*, 50–60. https://doi.org/10.1016/j.bpobgyn.2018.01.006.
Pluchino, N., Taylor, H.S., 2016. Endometriosis and Stem Cell Trafficking. Reprod. Sci. (Thousand Oaks, Calif.) *23* (12), 1616–1619. https://doi.org/10.1177/1933719116671219.
Polat, S., Yazir, Y., Duruksu, G., Kiliç, K.C., Mert, S., Gacar, G., Öncel Duman, B., Halbutoğullari, Z.S., 2024. Investigation of the differentiation potential of pericyte cells as an alternative source of mesenchymal stem cells. Acta Histochem. 126 (3), 152145 https://doi.org/10.1016/j.acthis.2024.152145.
Rei, C., Williams, T., Feloney, M., 2018. Endometriosis in a Man as a Rare Source of Abdominal Pain: A Case Report and Review of the Literature. Case Rep. Obstet. Gynecol. *2018*, 2083121 https://doi.org/10.1155/2018/2083121.
Roshangar, L., Abdollahifard, S., Majdi, A., Zarrintan, A., Ghasemzade, A., Farzadi, L., Soleimani Rad, S., Soleimani Rad, J., 2013. Study of ultrastructure and apoptosis in the endometrium of women with or without endometriosis. Iran. J. Reprod. Med. *11* (5), 399–404.
Sakabe, I., Hu, R., Jin, L., Clarke, R., Kasid, U.N., 2015. TMEM33: a new stress-inducible endoplasmic reticulum transmembrane protein and modulator of the unfolded protein response signaling. Breast Cancer Res. Treat. *153* (2), 285–297. https://doi.org/10.1007/s10549-015-3536-7.
Sampson, J.A., 1927. Peritoneal endometriosis due to menstrual dissemination of endometrial tissue into peritoneal cavity. Am. J. Obstet. Gynecol. 14, 422–469.
Sarihan, M., Kasap, M., Akpinar, G., 2024. Streamlined Biotinylation, Enrichment and Analysis for Enhanced Plasma Membrane Protein Identification Using TurboID and TurboID-Start Biotin Ligases. J. Membr. Biol. *257* (1-2), 91–105. https://doi.org/10.1007/s00232-023-00303-y.
Sezer, Z., Ekiz Yilmaz, T., Gungor, Z.B., Kalay, F., Guzel, E., 2020. Effects of vitamin E on nicotine-induced lipid peroxidation in rat granulosa cells: Folliculogenesis. Reprod. Biol. 20 (1), 63–74. https://doi.org/10.1016/j.repbio.2019.12.004.
Shi-Peng, G., Chun-Lin, C., Huan, W., Fan-Liang, M., Yong-Ning, C., Ya-Di, Z., Guang-Ping, Z., Ye-Ping, C., 2017. TMED2 promotes epithelial ovarian cancer growth. Oncotarget *8* (55), 94151–94165. https://doi.org/10.18632/oncotarget.21593.
Siva, A.B., Srivastava, P., Shivaji, S., 2014. Understanding the pathogenesis of endometriosis through proteomics: recent advances and future prospects. Proteom. Clin. Appl. *8* (1-2), 86–98. https://doi.org/10.1002/prca.201200082.
Spano, D., Colanzi, A., 2022. Golgi Complex: A Signaling Hub in Cancer. Cells *11* (13), 1990. https://doi.org/10.3390/cells11131990.
Stephani, M., Picchianti, L., Gajic, A., Beveridge, R., Skarwan, E., Sanchez de Medina Hernandez, V., Mohseni, A., Clavel, M., Zeng, Y., Naumann, C., Matuszkiewicz, M., Turco, E., Loefke, C., Li, B., Dürnberger, G., Schutzbier, M., Chen, H.T., Abdrakhmanov, A., Savova, A., Chia, K.S., Dagdas, Y., 2020. A cross-kingdom conserved ER-phagy receptor maintains endoplasmic reticulum homeostasis during stress. eLife *9*, e58396. https://doi.org/10.7554/eLife.58396.
Wang, D.Y., Abbasi, C., El-Rass, S., Li, J.Y., Dawood, F., Naito, K., Sharma, P., Bousette, N., Singh, S., Backx, P.H., Cox, B., Wen, X.Y., Liu, P.P., Gramolini, A.O., 2014. Endoplasmic reticulum resident protein 44 (ERp44) deficiency in mice and zebrafish leads to cardiac developmental and functional defects. J. Am. Heart Assoc. *3* (5), e001018 https://doi.org/10.1161/JAHA.114.001018.
Zhang, H., Niu, Y., Feng, J., Guo, H., Ye, X., Cui, H., 2006. Use of proteomic analysis of endometriosis to identify different protein expression in patients with endometriosis versus normal controls. Fertil. Steril. *86* (2), 274–282. https://doi.org/10.1016/j.fertnstert.2006.01.028.
Zuk, P.A., Zhu, M., Ashjian, P., De Ugarte, D.A., Huang, J.I., Mizuno, H., Alfonso, Z.C., Fraser, J.K., Benhaim, P., Hedrick, M.H., 2002. Human adipose tissue is a source of multipotent stem cells. Mol. Biol. Cell *13* (12), 4279–4295. https://doi.org/10.1091/mbc.e02-02-0105.